NTNU

Norwegian University of
Science and Technology

An Experimental and Numerical Study of Diffusion and Electrical Conductivity in Porous Media

Hedda Henriksdatter Blytt

Petroleum Geoscience and Engineering
Submission date: June 2017
Supervisor: Carl Fredrik Berg, IGP

Norwegian University of Science and Technology
Department of Geoscience and Petroleum

Acknowledgement

I would really like to extend my gratitude to my supervisor, Carl Fredrik Berg, for all the feedback, guidance and interesting discussion during my work on this master thesis. I am very thankful for all the time he has spent on helping me with this thesis.

I would like to thank Roger Overå for all the assistance and help in the laboratory. He was always available when needed, and explained everything very good. I would also like to thank Åge Siveretsen for providing me with the resistivity apparatus and the data program for reading and saving the data from the apparatus.

A big thanks to my family, especially my parents, for all the support through my five years at NTNU. Finally, a special thanks to all of my friends and classmates for making these five years so great, both social and academic.

Hedda Henriksdatter Blytt

Trondheim, June 2017

Abstract

In this Thesis the effective diffusion coefficient, the diffusibility and the formation factor in a porous medium are studied by preforming a diffusion experiment and electrical conductivity measurements. The main purpose is to compare the formation factor calculated from an electrical resistivity measurement with the reciprocal diffusibility estimated from diffusion experiments.

There is clearly an analogy between the diffusion of molecules and the electrical conductivity in the fluid phase of porous medium. Both equations are dependent on the same parameters, so the diffusibility and the formation factor calculated from these experiments should in theory be equal, when we disregard the excess of conductivity outside the water phase.

Almost all kind of siliclastic formations contain a certain amount of clay minerals, and clay minerals are conductive, though rocks usually are non-conductors. When there are clay minerals present in a formation it will increase the conductivity, because there will be more paths for the electrical charged ions to pass through than just in the pure pore space of the rock. On the contrary a diffusion process of molecules can only happen in the pore space of the rock. When clays are present in a formation, this will decrease the resistivity readings and reduce the formation factor. When resistivity logs are used to estimate the hydrocarbon content, it is essential to distinguish brine conductance from clay conductance.

The resistivity measurement is preformed by using a standard resistivity apparatus, while the diffusion experiment is custom made. The diffusibility and the effective diffusion coefficient from the diffusion experiments are found by matching the experimental data with numerical simulations. The difference between the reciprocal diffusibility and the formation factor should correspond to the increased conductance due to the presence of clay. The purpose of this work is to try to show that the formation factor calculated from resistivity measurement is lower than the formation factor estimated from diffusion, unfortunately the results unexpected.

Sammendrag

I denne masteroppgaven har den effektive diffusjons koeffisienten, formasjonsfaktoren og diffusibiliteten i sandstein blitt studert. Dette har blitt gjort ved å utføre et diffusjons eksperiment, samt målinger av konduktiviteten over en sandteins kjerne. Hovedmålet med oppgaven er å sammenligne formasjonsfaktoren estimert fra konduktivitetsmålinger med den gjensidige diffusibiliteten estimert gjennom flere diffusjons forsøk.

Det er påvist en tydelig sammenheng mellom diffusjon og konduksjon av ioner i fluider i porøse medium. Så i teorien burde formasjonsfaktoren og diffusibiliteten estimert i de to forskjellige eksperimentene bli like, når man ser bort i fra konduktiviteten av ioner utenfor pore volumet (i leirmineraler).

I nesten alle klastiske (sandsteins) formasjoner finner man mer eller mindre innhold av leire. Leirinnholdet påvirker resistiviteten, siden leirpartikler er konduktive. Dess mer en formasjon inneholder leire dess mer vil resistiviteten/formasjonsfaktoren til formasjonen minke. Resistivitetslogger er ofte essensielle når man skal vurdere hvilke soner som kan inneholde hydrokarboner, siden hydrokarbonfylte soner er mer resistive enn vannfylte soner. Derfor er det essentielt å vite leireinnholdet i de forksjellige formasjonene, sånn at dette kan korrigeres for.

Resistivitetsmålingene i denne oppgaven er gjort med et standard resistivitets apparat, mens diffusjons eksperimentene er egen designet. Diffusibiliteten og den effektive diffusjons koeffisienten er estimert ved å sammenligne den eksperimentelle kruven med data fra numeriske simuleringer. Forskjellen mellom formasjonsfaktoren og den gjensidige diffusibiliteten burde stemme med den økte konduktivitet forårsaket av at prøvesamplene av sandsteinen inneholder leire. Formålet med dette arbeidet er å prøve å vise at formasjonsfaktoren beregnet ut i fra resistivitetsmålingene er lavere enn formasjonsfaktoren estimert fra diffusjon, dessverre var resultatene ikke som forventet.

Contents

Acknowledgement i

Abstract iii

Sammendrag v

List of Figures xi

List of Tables xv

1 Introduction 1

1.1 Structure of This Master Thesis 2

2 Diffusion and Electrical Conductivity in Porous Media 3

2.1 Diffusion 3

2.1.1 Diffusion at the Pore Scale 3

2.1.2 Diffusion in Porous Media 6

2.2 Electrical Conductivity 8

2.2.1 Electrical Conductivity at the Pore Scale 8

2.2.2 Electrical Conductivity in Porous Media 9

2.3 The Analogy between Diffusion and Electrical Conductivity 11

2.4 The Effect of Conductive Solids 12

3 Experimental Preparations and Procedures 15

3.1 The Core 15

3.2 Cleaning of the Core 17

3.3 Core Plug Data 18
3.4 Porosity 19
3.5 Formation Factor 21
3.6 The Saltwater Solution 22

4 The Experiment **23**
4.1 Set Up 23
4.1.1 Unsteady State 24
4.1.2 Steady State 25
4.2 Processing of the Experimental Data 26

5 Matlab Implementation **29**
5.1 Unsteady State Solution 32
5.1.1 The Conjugate Gradient Method 34
5.1.2 Validation of the Unsteady State Code 36

6 Results and Evaluation **37**
6.1 Experimental Preparations Results 37
6.2 Results From the Diffusion Experiment 38
6.3 Validation of the Numerical Unsteady State Solution 41
6.4 Evaluation of the Diffusibility 43

7 Discussion **47**
7.1 Porosity 47
7.2 Formation Factor 48
7.3 Estimation of the Diffusibility from the Experimental and Numerical Data 48
7.4 The Effective Diffusion Coefficient and Formation Factor 54

8 Conclusion **59**
8.1 Further work 60

Nomenclature **61**

References **63**

Appendices **67**

A Analytical Solution to Fick's Second law **69**

B Resistivity for NaCl Solutions **71**

C Matlab Codes **73**

D Additional Results from Experiments **85**

E Risk Assessment **91**

List of Figures

2.1 Illustration of Fick's first law [9] in one dimension. 4
2.2 Illustration of the principle of the continuity equation [9]. 5
2.3 When salts are dissolved in water they split into an anion and a cation. These ions make up the basis of conductivity in water [13]. 8
2.4 The principle of the measurement of resistance in a solution [13]. 9
2.5 The three different distribution of clay particles in a porous rock [26]. . . 13

3.1 Scanning electron micrographs of a Berea sandstone showing the presence of fine-grained clay minerals partly filling pores between quartz grains [17]. 16
3.2 X-ray spectrum of clay minerals coating Berea Sandstone samples pores shown in figure 3.1. The nearly equal peaks of Si and Al confirms the identification of Kaolinite [17]. 16
3.3 Picture of the core samples used in this thesis. 17
3.4 Schematic diagram of a Soxhlet extraction [30]. 18
3.5 Schematic overview of the Helium Porosimeter apparatus [14]. 19
3.6 The electrical circuit used in the ratio of voltage decrease method, also see Figure 3.7, [14]. 21
3.7 The electrical circuit used in the ratio of voltage decrease method. Picture of the laboratory's apparatus. 22

4.1 Experimental setup for the unsteady state diffusion experiment, also see Figure 4.2. 24
4.2 Experimental setup for the unsteady state diffusion experiment. 25
4.3 Experimental setup for the steady state diffusion experiment. 26

4.4 Correlation curve for the *NaCl* concentration. 27

6.1 Resistivity in the water over the core sample for all the experiments. . . . 39
6.2 The flux stabilizes, which indicates a converge to a steady state solution. . 41
6.3 The concentration in the core when a steady state simulation is preformed. 42
6.4 The concentration in the core after the simulation is done. 42
6.5 The concentration of NaCl above the core sample from all of the experiments. 43
6.6 The plotted simulated resistivity for different Q values. 44
6.7 The plotted simulated concentration for different Q values.. 45

7.1 Resistivity in the water over the above core, experiment one and data from matlab simulations with different values of the diffusibility. 49
7.2 Concentration of *NaCl* in the water volume over the core, for experiment one and matlab simulations. 50
7.3 Resistivity of the water over the core plug, experiment two and matlab simulations with different diffusibility values. 50
7.4 Concentration of *NaCl* in the water above the core, experiment two and different numerical simulations. 51
7.5 Resistivity of the water above the core plug, experiment three and from matlab simulations with different Q values. 52
7.6 Concentration of *NaCl* in the water above the core plug, experiment three and simulated data. 52
7.7 Resistivity in the water above the core plug, experiment four and from the numerical simulations. 53
7.8 Concentration of *NaCl* in the water over the core plug, experiment four and simulated data. 54

D.1 Resistivity in the water over the core plug, Experiment one. 85
D.2 Resistivity in the water over the core plug, Experiment two. 86
D.3 Resistivity in the water over the core plug, Experiment three. 86
D.4 Resistivity in the water over the core plug, Experiment four. 87
D.5 Concentration of *NaCl* in the water above the core plug in experiment one 87
D.6 Concentration of *NaCl* in the water above the core plug in experiment two. 88

D.7 Concentration of *NaCl* in the water above the core plug in experiment three. 88
D.8 Concentration of *NaCl* in the water above the core plug in experiment four. 89

List of Tables

6.1 Core plugs data. 37
6.2 Data from the Helium Porosimeter measurements. 38
6.3 Results of the resistivity measurements 38
6.4 Data used to calculate the formation factor and the calculated formation factor. 39
6.5 Data from the experiments. 40

7.1 Formation factor and the effective diffusion coefficient from experiment two to four. 54

Chapter 1

Introduction

Electrical conductivity and diffusion are derived from the movement of particles in a material. Conduction is the movement of ions from a region of high concentration to a region of low concentration, *transport of electrons by random motion*. While diffusion is the movement of molecules from a region of high concentration to a region of low concentration, *transport of material by random motion*. So there is clearly an analogy between diffusion and electrical conductivity, both describes the movement of a substance down a concentration gradient [1] [2].

A reservoir rock is a porous media and consist mainly of minerals, grains and fluid filled pore space. The solid with exception of certain clay minerals are considered as non-conductive [3]. Thus diffusion and conductance can only happen in the pore space, where the conductive fluid flow. So both the effective diffusion and the effective conductance will be smaller than the parameters in a solute, because the available cross sectional area for particle flow is less due to more complex pathways in the porous medium [4] [5].

The distribution of clay minerals in the formations can have a large impact on the different logging tools, and may complicate the determination of saturation and porosity. Unlike other minerals in the rock, clays alter the conductivity of the formation so that a straightforward application of the Archie relation often gives a water saturation which are too high [6].

Since there exists an analogy between electrical conductance and diffusion in porous media, this can be used to compare the formation factor calculated from both measurements.

Both the diffusibility and the formation factor says something about the porosity and pore geometry in the porous media.

This thesis comprises both an unsteady state experiment and a numerical simulation to estimate the effective diffusion coefficient and the diffusibility in a sandstone core sample. The formation factor have been calculated from resistivity measurements, and also calculated from the effective diffusion coefficient measured in the sandstone. The plan was to do a steady state experiment as well, but this was not possible because the pump did not function at the low rate which the experiment needed.

1.1 Structure of This Master Thesis

The Thesis is structured into seven main Chapters:

- ***Chapter 2*** Describes the theory of diffusion and electrical conductivity at both pore scale and in the porous medium.
- ***Chapter 3*** Overview over the experimental preparations and procedures done to the core plugs.
- ***Chapter 4*** Describes the set up for the main experiment, both unsteady state and steady state, as well as explaining the processing of the experimental data.
- ***Chapter 5*** Description of how the numerical simulation is solved for unsteady state.
- ***Chapter 6*** An overview of the results obtained from the experiments and the numerical simulations.
- ***Chapter 7*** Discussion of everything presented in this master thesis, and comparison of the experiments and the numerical results.
- ***Chapter 8*** Presents the conclusion of this thesis and suggestion for further work.

Chapter 2

Diffusion and Electrical Conductivity in Porous Media

As stated in the introduction there is an analogy between diffusion and electrical conductivity in porous media. This section describes the theory of diffusion and electrical conductivity for both pore scale and in the porous medium.

2.1 Diffusion

Diffusion is the movement of molecules from a region of high concentration to a region of low concentration, in other words it is the movement of a substance down a concentration gradient [1]. When two miscible fluids are in contact with each another they will slowly diffuse into each another. The sharp interface between the two fluids will become diffuse as time passes [7].

2.1.1 Diffusion at the Pore Scale

A diffusion is time dependent, the amount of matter transferred depends on the time and is characterized by the diffusion flux [8], which is defined in Equation 2.1. The flux is defined as the rate of flow per unit area.

$$J = \frac{C}{At} = \frac{Mass}{area \cdot time}[g/cm^2 sec] \tag{2.1}$$

The diffusion process will eventually reach steady-state conditions, and the flux J in Equation 2.1, will no longer change with time. When steady state diffusion is reached, the diffusion process is described by Fick's first law, shown in Equation 2.2. Fick studied the concept of the diffusion coefficient and suggested a linear response between the concentration gradient and the mixing of salt and water [9].

It is assumed that the flux goes from regions of high concentration to regions of low concentration with a magnitude that is proportional to the concentration gradient [4]. Let us first consider the flux of diffusing particles in one dimension (x-direction) illustrated in Figure 2.1 [9].

$$J_x = -D\frac{\partial C}{\partial x} \tag{2.2}$$

Here J_x denote the flux of particles and C the concentration of particles, D is the diffusion coefficient and describes the rapidity with which the ions diffuse into the distilled water. The negative sign in Equation 2.2 indicates that the diffusion flux and concentration gradient are conversely proportional.

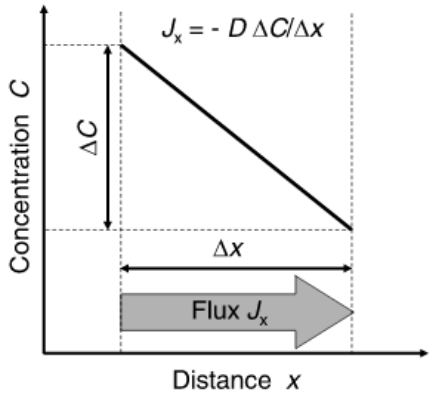

Figure 2.1: Illustration of Fick's first law [9] in one dimension.

Further on it is applicable to generalize Fick's first law to two or more dimensions using a vector notation, as shown in Equation 2.3.

$$J = -D\nabla C \tag{2.3}$$

The equation of continuity is then used to derive Fick's second law. The equation of continuity is an expression for material balance, which is expressed as:

$$inflow - outflow = \text{accumulation (or loss) rate} \tag{2.4}$$

This is done by choosing a random point P located at (x,y,z) and a reference volume size Δx, Δy and Δz, as shown in Figure 2.2. The diffusion flux J and its components J_x, J_y, J_z will vary across the test volume. If the sum of the fluxes over the test volume is not at balance, a net accumulation has occurred.

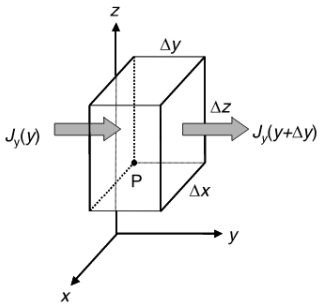

Figure 2.2: Illustration of the principle of the continuity equation [9].

The flux components can be substituted into Equation 2.4 [9]:

$$-[\frac{\partial J_x}{\partial x} + \frac{\partial J_y}{\partial y} + \frac{\partial J_z}{\partial z}]\Delta x \Delta y \Delta z = \frac{\partial C}{\partial t}\Delta x \Delta y \Delta z \tag{2.5}$$

The accumulation rate is expressed in terms of the partial time derivative of the concentration. For an infinity small test volume, Equation 2.5 can be written with the vector operation divergence ∇.

$$-\nabla \cdot J = \frac{\partial C}{\partial t} \tag{2.6}$$

Equation 2.6 is denoted as *the continuity equation*.

To get Fick's second law (*"the Diffusion Equation"*), Fick's first law, Equation 2.2, is combined with the equation of continuity, Equation 2.6.

$$\frac{\partial C}{\partial t} = \nabla \cdot (D \nabla C) \tag{2.7}$$

Since this experiment is a tracer diffusion in a chemically homogeneous system, the diffusivity is independent of the concentration, and Equation 2.7 simplifies to:

$$\frac{\partial C}{\partial t} = D\Delta C \tag{2.8}$$

Δ denotes the Laplace operator, and this form of Fick' second law is a linear second-order partial differential equation for the concentration field $C(x,y,z,t)$. However, Equation 2.8 only yields for diffusion at the pore scale, when there is a diffusion in a porous medium it can be dependent on the location in the porous medium.

2.1.2 Diffusion in Porous Media

A porous medium is characterized by a partitioning of the total volume into solid matrix and pore space [10]. Since the diffusion happens by fluid movement, the connected pore space in the porous media is what is interesting. The diffusion coefficient in a porous media is obviously smaller than the bulk diffusion coefficient, because the cross sectional area will be smaller and this will slow down the diffusion process. Therefore, an effective diffusion coefficient is proposed, which is based on the average cross sectional area open for diffusion and variation in pore size along the diffusion path (the average fieldlines and velocity along the effective pathways) [11]. The effective diffusion coefficient is assumed not to depend on the concentration, but it may depend on flow rate (in this case zero) and fluid properties [12].

The relationship between the diffusion coefficient and the effective diffusion coefficient is called diffusibility , Q, defined in Equation 2.9. The diffusibility is defined as the quality of being diffusive or the capability of being spread out. The fluid can only be spread out in the pore spaces of the rock, so the relationship between the diffusion and the effective diffusion is obviously dependent of the porosity of the core sample, as well as it is dependent of the pore geometry.

$$\frac{D_e}{D} = Q \tag{2.9}$$

If we substitute for D in Equation 2.7, we get the diffusion equation for a porous media.

$$\phi \frac{\partial C}{\partial t} = DQ\nabla^2 C \tag{2.10}$$

In this thesis we look at two different diffusions; steady state and unsteady state. If there is steady state conditions there are no change of concentration with time, so Equation 2.10 simplifies to Equation 2.11, which apply for one dimension.

$$\frac{\partial C}{\partial t} = 0 \qquad = \qquad \frac{DQ}{\phi}\frac{\partial^2 C}{\partial x^2} = 0 \tag{2.11}$$

With the solution:

$$C(x) = Ax + a \tag{2.12}$$

A and a denote constants in Equation 2.12. The diffusion coefficient is assumed to be constant, so under linear flow steady-state conditions the concentration gradient will be constant (in this case the constant A) [9]. $C(x)$ and the flux J is defined by Equation 2.13 and 2.14.

$$C(x) = C_1 + \frac{C_2 - C_1}{L_x}x \tag{2.13}$$

$$J = \frac{AD}{\phi F}\frac{C_1 - C_2}{L_x} \tag{2.14}$$

An unsteady state diffusion describes a process where the diffusion flux and the concentration changes with respect to time, this can be solved by using Fick‘s second law. Fick’s second law for one dimensional diffusion is stated in Equation 2.15.

$$\frac{\partial C}{\partial t} = \frac{D_e}{\phi}\frac{\partial^2 C}{\partial x^2} \tag{2.15}$$

To derive a solution to Equation 2.15 a set of boundary conditions have to be defined:
For $t = 0, C = C_0$ at $0 < x < \infty$
For $t = 0, C = C_s$, the constant concentration at $x = 0$
$C = C_0$ at $x = \infty$
These boundary conditions applies for the start of the unsteady state experiment only, and are used as an example only.

Including these three boundary conditions, the solution to Fick’s second law is shown in

Equation 2.16, the step by step solution is shown in Appendix A:

$$\frac{C_x - C_0}{C_s - C_0} = erf(\frac{x}{2\sqrt{Dt}}) \tag{2.16}$$

erf is an error function, which only can be represented by an integral.

2.2 Electrical Conductivity

Electrical conductivity is the movement of ions from a region of high concentration to a region of low concentration, in other words it is the movement of a substance down a concentration gradient [1].

2.2.1 Electrical Conductivity at the Pore Scale

Conductivity is a measurement of a material capability to pass electrical flow, which is directly related to the concentration of ions in the material. The conductive ions come from dissolved salts or inorganic materials such as chlorides, sulfides and carbonate compounds. The higher the concentration of ions the higher the conductivity and vice versa. Ions are conductive because of their positive and negative charges, see Figure 2.3 [13]. Conductivity is often calculated from the resistivity, which is the inverse of

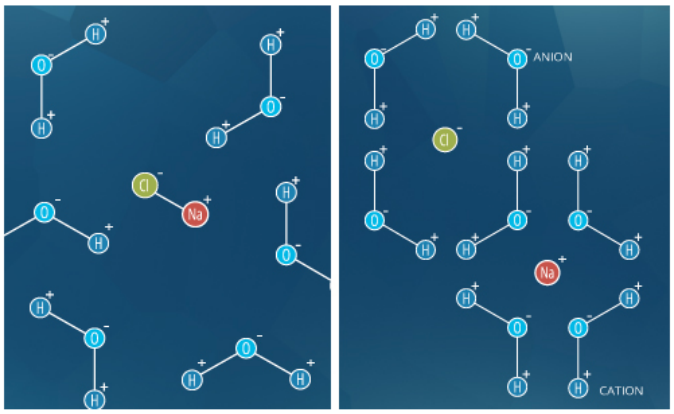

Figure 2.3: When salts are dissolved in water they split into an anion and a cation. These ions make up the basis of conductivity in water [13].

conductivity. The conductivity of a solution is measured by determining the resistance of the solution between two electrodes separated by a fixed distance, as shown in Figure 2.4. The resistance is measured by a resistivity meter.

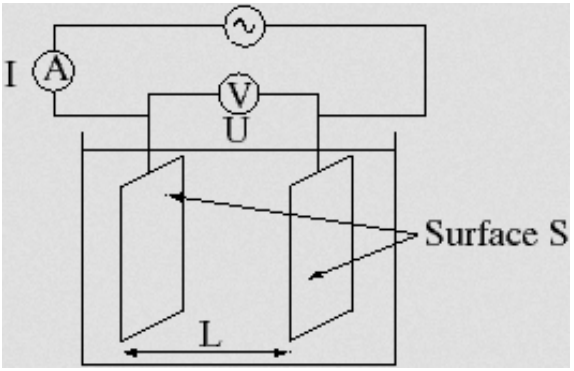

Figure 2.4: The principle of the measurement of resistance in a solution [13].

The resistance is inversely proportional to the distance, l, between the electrodes and proportional to the cross sectional area of the sample. The definition of resistivity is given in Equation 2.17.

$$R = \frac{Ar}{L} \tag{2.17}$$

2.2.2 Electrical Conductivity in Porous Media

Rocks are usually non-conductive, unless they contain some clay minerals. For a rock sample with small amounts of clay there is mainly the pore fluid which carries the current. The resistivity of the rock depend on the following properties: Porosity, pore fluid resistivity (salinity), temperature, pore fluid saturation, clay content and pressure. In this thesis it is focus on the conduction due to the pore fluid resistivity and clay content [3]. The fluids of interest in a reservoir rock are oil, gas and water. Oil and gas are nonconductors and water is conductive when it contains dissolved salts, such as $NaCl$, $MgCl_2$, KCl [3] [14].

The resistivity to the rock is measured by saturating the rock with a conductive solution and then measure the resistance both of the saturated rock [R_o] and of the pore fluid [R_w], then the resistivity can be calculated by using Equation 2.17. The *Formation Resistivity Factor* is the most fundamental concept in considering electrical properties of a rock, as

defined by Archie [15].

$$F = \frac{R_o}{R_w} = \frac{\sigma_w}{\sigma_o} \tag{2.18}$$

The formation factor characterizes the solids microstructure since the only difference between the conductivities are due to the restricted pathways through which the current is constrained in the bulk conductivity measurement [16].

There are a lot of assumptions that apply for the formation factor concept;
1. The conduction process is electrolytic and it occurs only through the pore network where there is solution present.
2. The properties of the solution filling the pores are uniform,
3. There are no surface conductivity effects.
If this was true, the plot of the electrical conductance of the solution versus the electrical conductance of the rock saturated with the solution would be a straight line passing through the origin [17]. The formation factor calculated by Equation 2.18 is applicable or true only for clean or clay-free minerals [18] [19].

Since the formation factor shows a relationship between water saturated rock conductivity and bulk water conductivity, it is obviously dependent of the pore structure of the rock. So the formation factor gives an indication of the influence the pore structure has on the resistance of the rock sample. If there is none conductive mineral layers the current can flow through the fluid in the rocks interconnected pores only. This implies that F is related to the porosity of the rock [14] [3].

The formation factor value is dimensionless and will always be greater than one. The pore structure in a rock influence the conductivity in two different ways: the reduction of the cross section which is available for conduction and the orientation and length of conduction path. For isotropic disordered media, the ratio of the cross section available for conduction to the bulk cross section is equal to the bulk porosity [20]. So the formation factor is inversely related to the porosity, as shown by Archie [15] who purposed Equation 2.19.

$$F = \phi^{-m} \tag{2.19}$$

Berg [21] developed another relation between the formation factor and the porosity, which

includes the tortuosity. Tortuosity is a ratio that characterizes the pathways of fluid diffusion and electrical conduction through porous media [22]. Based on simple pore models Equation 2.20 can be derived.

$$F = \frac{1}{\phi \tau^2} \tag{2.20}$$

2.3 The Analogy between Diffusion and Electrical Conductivity

There is clearly an analogy between diffusion and electrical conductivity in porous media. Fick's law, Equation 2.21, is analogous to Ohm's law, Equation 2.22.

$$J = -D\nabla C \tag{2.21}$$

$$J = -\sigma\nabla V \tag{2.22}$$

Fick's law describes the transport of particles, while Ohm's law the transport of electric charge. Since both equations are dependent of exactly the same parameters, the solutions will be equal. From comparing the electrical conductivity in the pore space and in the porous media we got the relationship defined as the formation factor, from Equation 2.18. Since the diffusion equation is dependent of the same parameters, we get the same relationship for the formation factor by the difference of diffusion in the pore space and diffusion in a porous medium.

$$\frac{1}{Q} = F$$

So the formation factor calculated from electrical conductivity and from diffusion in porous media should in theory be equal.

$$\frac{\sigma}{\sigma_e} = \frac{D}{D_e} = F$$

This is only accurate if the porous media do not contain any clay minerals, which is rarely.

2.4 The Effect of Conductive Solids

Clays are minerals with high porosities and very low permeabilities. The minerals themselves may not be very conductive, but their surface causes an excess of cations in the pore fluid immediately adjacent to the clay surfaces. This will cause a higher conductivity near the clay surfaces, which may dominate the overall conductance if the pore water conductivity is low [23] [18].

The clay content in a rock can be divided into three types;
1. Dispersed clay, which means that the clay particles are dispersed on the surface of the matrix, in other words clay particles occupying the pore space. Dispersed clay will decrease the effective porosity and increase the conductivity.
2. Structured clay, the clay particles are an original part of the matrix and will not have any huge effect on the porosity, but it will most likely have an effect on the conductance of the rock.
3. Laminated clay, the clay particles are distributed in a form of a layer replacing space of matrix and pore in the rock [24]. If there is laminated clay in the formation this will mainly have an effect on the vertical conductivity, and to do less extent on the horizontal conductivity. So if there is any laminated clay this will effect the log readings, but this experiment is on a very small scale, so the laminated clay will not have any special impact on the conductivity measurements.
The different distributions are schematically illustrated in Figure 2.5 [16].

Many downhole log measurements and readings are affected by clay in the formation, so a reliable evaluation of the clay content is essential in formation evaluation from logs [25]. Clay minerals are almost always present in different formations, not only in shale beds, but also in most of the reservoir rocks. The clay content will most likely have an effect on all the downhole logs, but the electrical ones are the most impacted. So when the different formations are studied for potential hydrocarbon content it is important to have a reliable estimation of the clay content in the formation [25].

The presence of clay in the formation will decrease the resistivity on the resistivity logs, and maybe decrease the apparent hydrocarbon saturation (oil and gas have a high resistivity,

non-conductors). The degree of the effect the clay content will do is dependent on the volume of the clay and the distribution of the clay [26] [24].

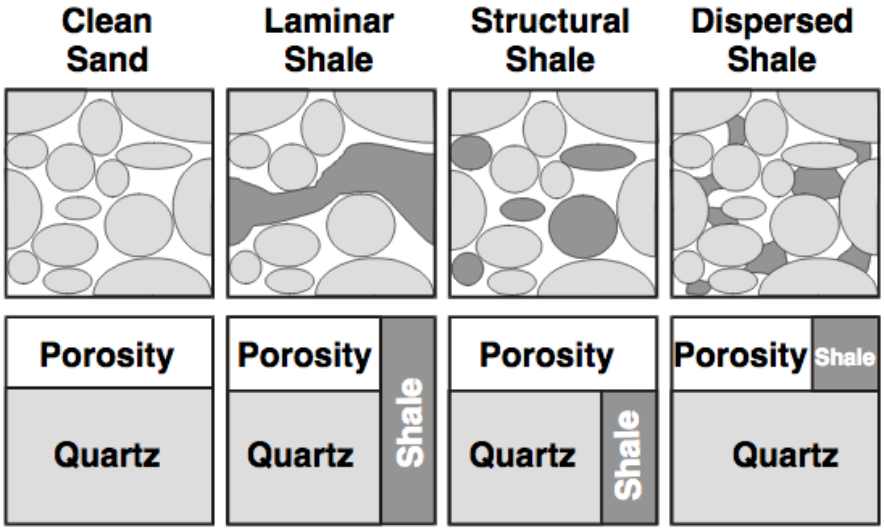

Figure 2.5: The three different distribution of clay particles in a porous rock [26].

Chapter 3

Experimental Preparations and Procedures

Before the main experiment was preformed some experimental preparations and procedures had to be done. The core sample had to be cleaned and cut in the right size. Some important properties for the core sample had to be measured before it got saturated with brine or distilled water.

3.1 The Core

The core used in this experiment is the Berea sandstone, which is widely recognized by the petroleum industry as one of the best stones for testing. The Berea Sandstone is a sedimentary rock whose grains are sand-sized and are composed of quartz held together by silica. The Berea sandstones usually has high porosity and permeability and represents a good reservoir rock [27].

A Berea sandstone usually contains between zero and 15 % of clay minerals, which are coating the available pore space [17] [28] [29]. Studies done by Khilar and Fogler [17], with scanning electron microscopy (shown in Figure 3.1) and energy dispersive x-ray analysis (shown in Figure 3.2) indicate that the Berea rock contains about 8% of dispersable and swelling clays (mainly kaolinite, and some illite and smectite).

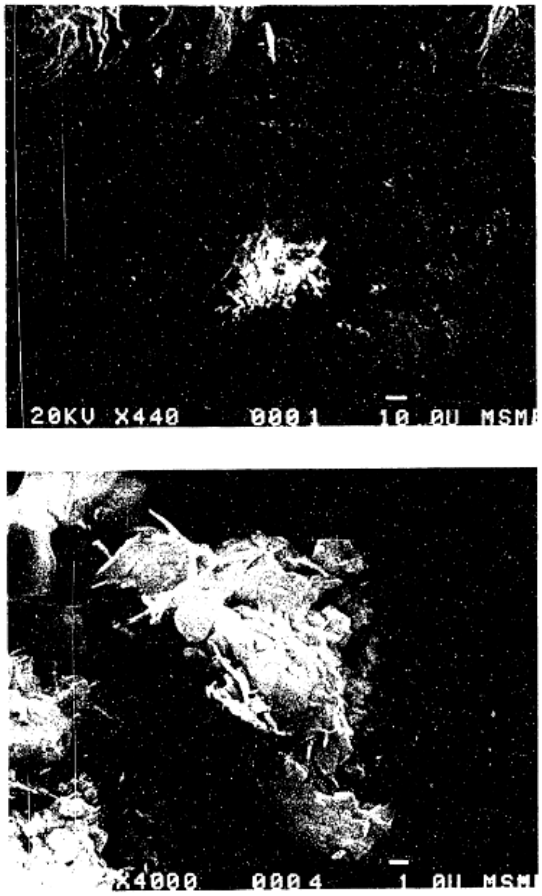

Figure 3.1: Scanning electron micrographs of a Berea sandstone showing the presence of fine-grained clay minerals partly filling pores between quartz grains [17].

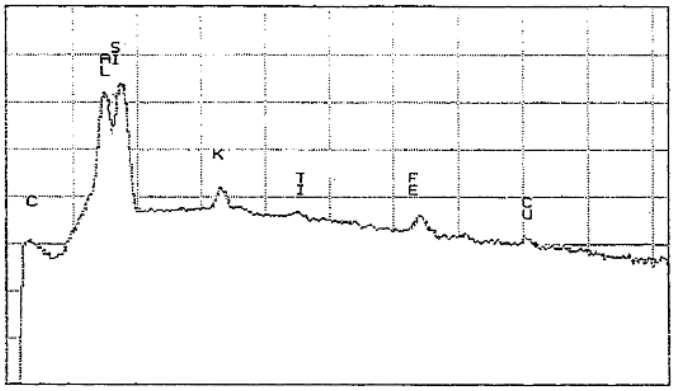

Figure 3.2: X-ray spectrum of clay minerals coating Berea Sandstone samples pores shown in figure 3.1. The nearly equal peaks of Si and Al confirms the identification of Kaolinite [17].

The diffusion coefficient for $NaCl$ in water is around $2 \times 10^{-9}\ m^2/sec$, so the diffusion process is slow. Therefore it was essential to have a thin enough core plug, so that the

experiment would not take several weeks or even months. It was decided to try to cut the core into 5 mm plugs, and it ended up to be five core samples with the length of approximately 6 mm. There was also need for a regular length core, because the 6 mm cores were so small to fit in the lab's resistivity measurement apparatus and in the Helium Porosimeter. Thus a core sample with a length of 40 mm was used to measured this properties. In figure 3.3 the two different core plugs are shown.

Figure 3.3: Picture of the core samples used in this thesis.

3.2 Cleaning of the Core

It is important to clean the cores of residual fluids before they are used in this experiment. To get the cores properly cleaned a Soxhlet extraction was done, which is a continuous solid/liquid extraction [14].

The core is placed in the thimble, see Figure 3.4, the thimble is made of a material which will allow the liquids to pass through (a kind of filter paper). The thimble with the core is placed in the Soxhlet extractor, and toluene/methane is then heated to a slow boil in a Pyrex flask. As it boils the vapor ascend and the condensed solvent will fill up the thimble. Eventually the solvent, in this case water, within the core sample will be vaporized. The extraction solvent and the solvent from the core vapors enter the inner chamber of the condenser, and the cold water circulating around the inner chamber condenses both vapors

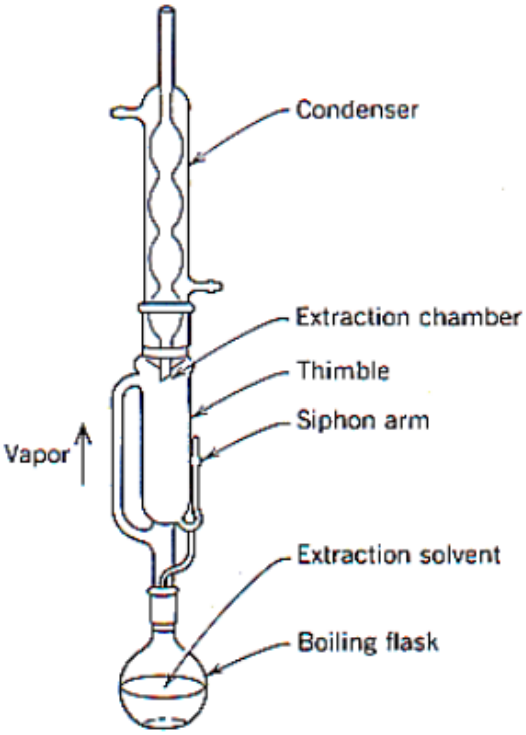

Figure 3.4: Schematic diagram of a Soxhlet extraction [30].

to immiscible liquids. Recondensed toluene and water falls down onto the core sample in the thimble; the toluene soaks the core sample and dissolves any oil with which it come into contact. When the liquid level within the Soxhlet tube reaches the top of the siphon tube arrangement, the liquids within the Soxhlet tube are automatically emptied by a siphon effect and flow into the boiling flask. The extraction solvent is then ready to start another cycle [30] [14].

A throughout extraction may take several days or even weeks in case of low API gravity crude or presence of heavy residual hydrocarbon deposit within the core. The cores used in this experiment was quite new, so it took only a couple of days.

3.3 Core Plug Data

After the core plugs were cleaned and dried, the plugs length and diameter were measured by using a caliper. All of the core plugs came originally from one core sample, but were

cut in different pieces in the lab.

3.4 Porosity

The porosity is defined as the percentage of the pore volume of the bulk volume to a porous media. Porosity can be divided into two different groups; total porosity and effective porosity. The total porosity is defined as the total pore volume, and is defined by Equation 3.1.

$$\phi = \frac{\text{pore volume}}{\text{bulk volume}} \tag{3.1}$$

The effective porosity is the ratio of interconnected pore spaces to the bulk volume. Thus, only the effective porosity contains fluids that can be produced from wells. The effective porosity in the Berea sandstone was determined by using the Helium Porosimeter method, which is shown schematically in Figure 3.5.

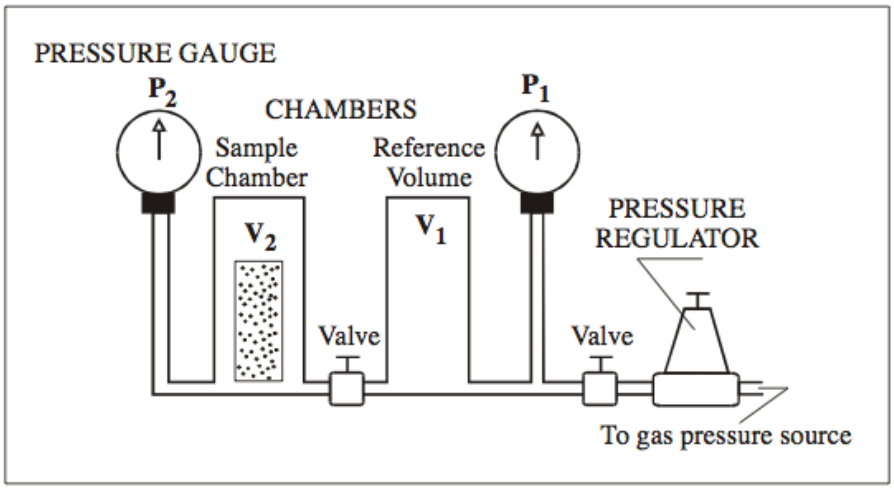

Figure 3.5: Schematic overview of the Helium Porosimeter apparatus [14].

The Helium Porosimeter is one of the most used methods to determine the effective porosity because of four advantages:

1. The small molecules can easily penetrate the small pores in the rock sample.
2. Helium is an inert gas, and will not be adsorbed on the rock surface.
3. Helium is considered as an ideal gas for pressures and temperatures.

4. Helium has a high diffusivity, which is useful when determining porosity for low permeability rocks.

The helium porosimeter use the principle of gas expansion, as described by Boyle's law [14]:

$$P_1V_1 = P_2V_2 \tag{3.2}$$

Boyle's law, Equation 3.2), describes the inverse relationship between the volume and pressure of a fixed amount of gas in isothermal conditions [31]. A known reference cell volume of helium gas is isothermally expanded into a sample chamber, and the equilibrium pressure is measured. The measured pressure depends on the volume of the sample chamber minus the rock grain volume, and the porosity can be found [14].

The Helium porosimeter has a reference volume V_1 at pressure p_1, and a matrix cup with an unknown volume V_2 and initial pressure p_2, as shown in figure 3.5. The two cells are connected by a tubing, and the system is brought to equilibrium when the core holder valve is opened, and determination of the unknown volume V_2 by measuring the resultant equilibrium pressure p. When this valve is opened the volume of the system will be the sum of V_1 and V_2. Since the expansion takes place under isothermally condition, Boyle's law is applied:

$$p_1V_1 + p_2V_2 = p(V_1 + V_2) \tag{3.3}$$

After the Helium Porosimeter procedure is done, the effective pore volume is calculated by using Equation 3.4 and 3.5.

$$V_m = V_1 - V_2 \tag{3.4}$$

$$\phi = \frac{V_b - V_m}{V_b} \tag{3.5}$$

Where V_b is the cores bulk volume.

3.5 Formation Factor

To calculate the formation factor to the Berea Sandstone, the resistivity of the rock has to be measured. To do this the method applied is the ratio of voltage decrease method, which is the ratio of voltage decrease between a reference resistor and a sample in series, see Figure 3.6 [14].

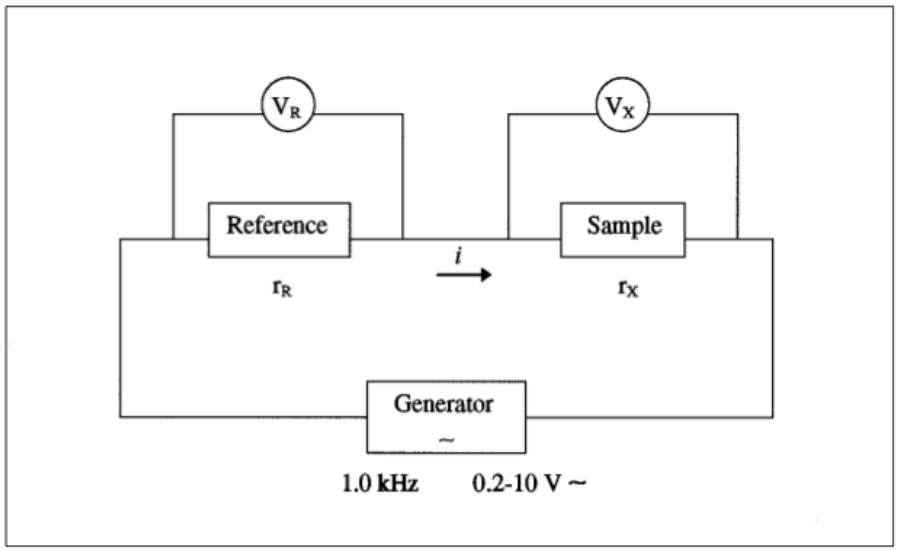

Figure 3.6: The electrical circuit used in the ratio of voltage decrease method, also see Figure 3.7, [14].

Further on Ohm's law, Equation 3.6, is used to calculate the resistivity of the the rock fully saturated with saltwater.

$$U = IR \tag{3.6}$$

$$\frac{U_x}{r_x} = \frac{U_r}{r_r} \qquad \text{and} \qquad r_x = \frac{U_x r_r}{U_r} \tag{3.7}$$

After U_x and U_r are measured using the apparatus shown in Figure 3.6 and r_x is calculated by using Equation 3.7, one can calculate the resistivity of the rock saturated with saltwater using Equation 2.17. Then calculate the formation factor by using Equations 2.18. R_w in Equation 2.18 is found in a conversion diagram provided by Schlumberger, the diagram is shown in Appendix B.

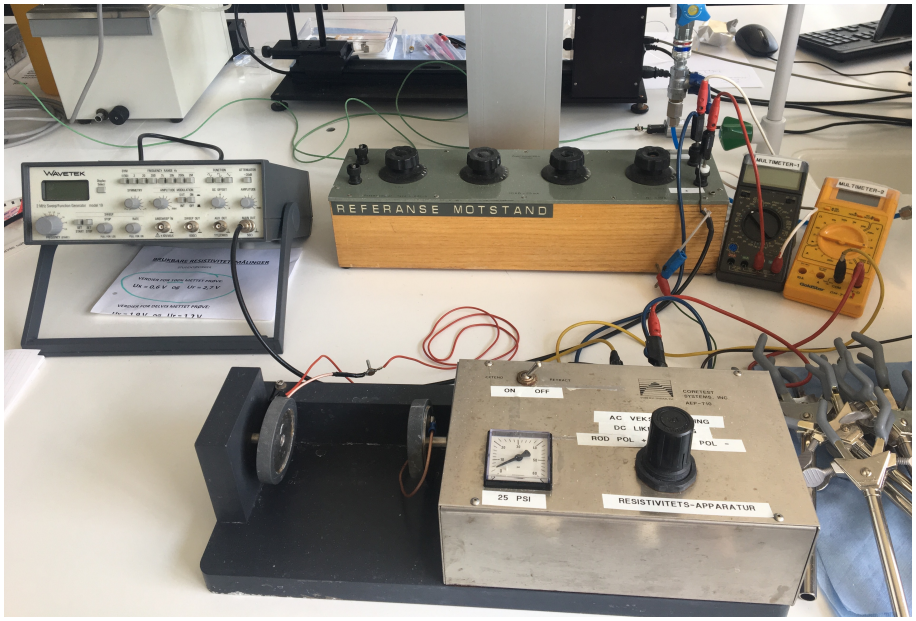

Figure 3.7: The electrical circuit used in the ratio of voltage decrease method. Picture of the laboratory‘s apparatus.

Figure 3.7 shows the laboratory‘s resistivity measurement apparatus.

3.6 The Saltwater Solution

To perform this experiment several liters of brine is needed. The brine was simply mixed by using distilled water and $NaCl$. For this experiment a brine with a concentration of 5% $NaCl$ was used. The saltwater was mixed in flasks with a volume of 2L, so for each flask there was $100g$ of $NaCl$.

Chapter 4

The Experiment

This is a sensitive, but quite simple, experiment. Once everything is in place, it is only to wait until the resistivity readings stabilize. The diffusion is through a Berea sandstone core plug, which is in contact with saltwater at one side and a small volume of distilled water at the other side.

4.1 Set Up

The core has to be fully saturated with distilled water before it is placed in the core sleeve. To saturate the cores place them in distilled water for at least one day. Saltwater of 5 wt% $NaCl$ is mixed, as described in Chapter 3.6, and then poured into the tank, see Figure 4.1 and 4.2.

The two electrodes from the resistivity apparatus have to be taped on each side of the core-sleeve, so they will keep the same distance during the experiment. Then connect the resistivity apparatus to the computer with an USB cable, and start the computer program which stores all the resistivity readings (since the computer and the program for the resistivity apparatus is quite old, it will use some time before they two are connected). Since the core plug is so thin and have a high porosity, it is a challenge to place the core without neither leak distilled water into the saltwater or prevent the saltwater to saturate the core before the volume over the core is filled with distilled water.

4.1.1 Unsteady State

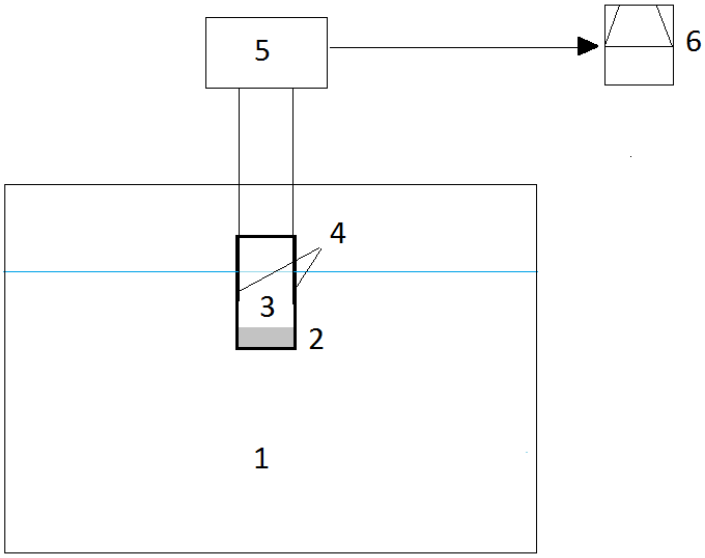

1) Saltwater with 5 wt% NaCl
2) The core sample in a sleeve
3) Distilled water
4) Electrodes
5) Resistivity apparatus
6) Computer

Figure 4.1: Experimental setup for the unsteady state diffusion experiment, also see Figure 4.2.

The set up for the unsteady state experiment is shown in Figure 4.1 and 4.2. For the unsteady state experiment, the volumes over and under the core are steady. Fill the tank with saltwater until the water surface is just beneath the core holder. Have a flask of 2L extra brine, that will have to be poured in as soon as the core is in place. This is important so that there is no pressure difference, then the distilled water may diffuse through the core and into the saltwater.

Secure the two electrodes right over the core inside the core-sleeve, and turn on the resistivity apparatus. Put the core 100 % saturated with distilled water inside the core-sleeve and place the core-sleeve with the core and the electrodes in the core holder. Do not push it all the way down to the saltwater surface at once! Fill it (around 20 mL) with distilled water, and push the core-sleeve down in the saltwater and pour the extra 2L with saltwater into the tank, so that the saltwater surface and the distilled water surface inside the sleeve is at the same level. Leave the core in this condition for a couple of days, until the

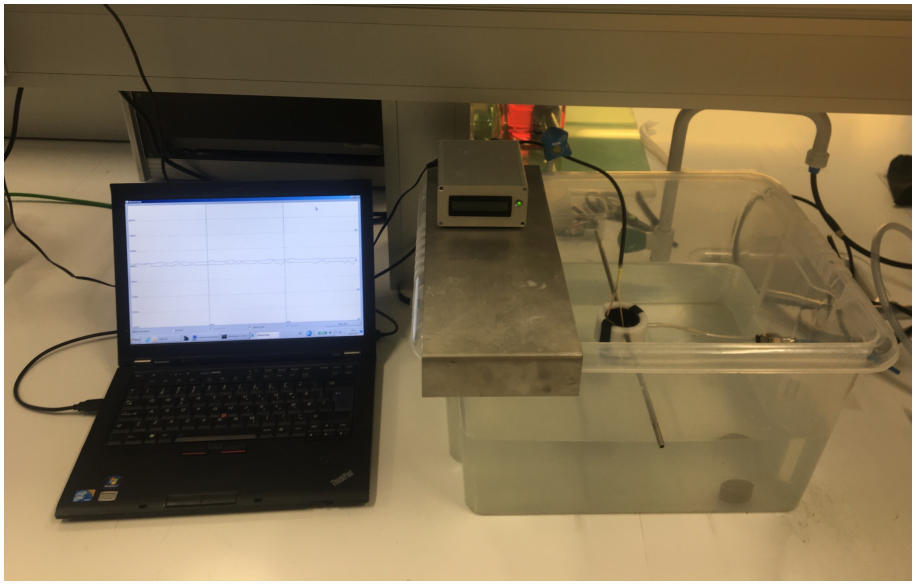

Figure 4.2: Experimental setup for the unsteady state diffusion experiment.

resistivity reading stabilizes over a significant period of time.

4.1.2 Steady State

This is a sensitive experiment, and the rate over the core in testing will most likely have to be very low. This is because the diffusion process will take time, even if the core has a thickness of only 0.6 cm. The flow rate over the core is calculate as:

$$q_{core} = D_e \nabla C A' \tag{4.1}$$

Where q_{core} is the rate, D is a given diffusion constant for $NaCl$ in water at 20 degrees, and A' is the effective cross-sectional area:

$$D_e = \frac{D}{F}$$

$$A' = \pi r^2 cm^2 \phi$$

$$\nabla C = \frac{\Delta C}{\Delta x}$$

After the pump rate is estimated the experiment can start, the set up is shown in Figure 4.3. As mentioned in the introduction the steady state experiment was not preformed for

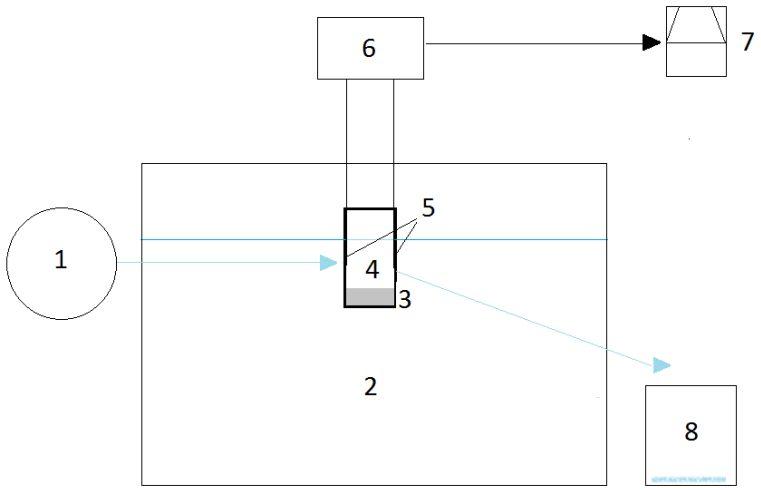

1) Pump
2) Saltwater with 5wt% NaCl
3) The core sample in a sleeve
4) Distilled water
5) Electrodes
6) Resistivity apparatus
7) Computer
8) Accumulated water with NaCl

Figure 4.3: Experimental setup for the steady state diffusion experiment.

this thesis, because the pump did not work at the desired rate.

4.2 Processing of the Experimental Data

To calculate the concentration over the core, we need to know what resistivity value correlates to what concentration. Conductance and concentration have a linear relationship. The conductance is the inverse of the resistance:

$$\sigma = \frac{1}{\rho} \tag{4.2}$$

When the resistance is converted to the conductance, one can convert the conductance to the concentration of salt. Do a series of resistivity measurements on salt solutions with concentrations that are already known. Then plot the relation between salt concentration and the solutions conductance. Then one can measure the conductance in an unknown solution, and calculate the concentration from the measured conductance value. The minimum concentration of salt, which is in the distilled water over the core, is known

to be around 0.5 wt% and the maximum salt concentration is 5 wt%. The concentration is easily converted to g/cm^3 by this equation:

$$C_{NaCl}[g/cm^3] = \frac{C_{NaCl}[wt\%]}{\frac{C_{NaCl}[wt\%]}{\rho_{NaCl}[g/cm^3]} + \frac{C_{H_2O}[wt\%]}{\rho_{H_2O}[g/cm^3]}} \tag{4.3}$$

By measuring the conductance to these two known concentrations and the plot them (Figure 4.4), an equation for the concentration can be derived. When this is done it is important to have a fixed distance between the two electrodes, this apply for the whole experiment.

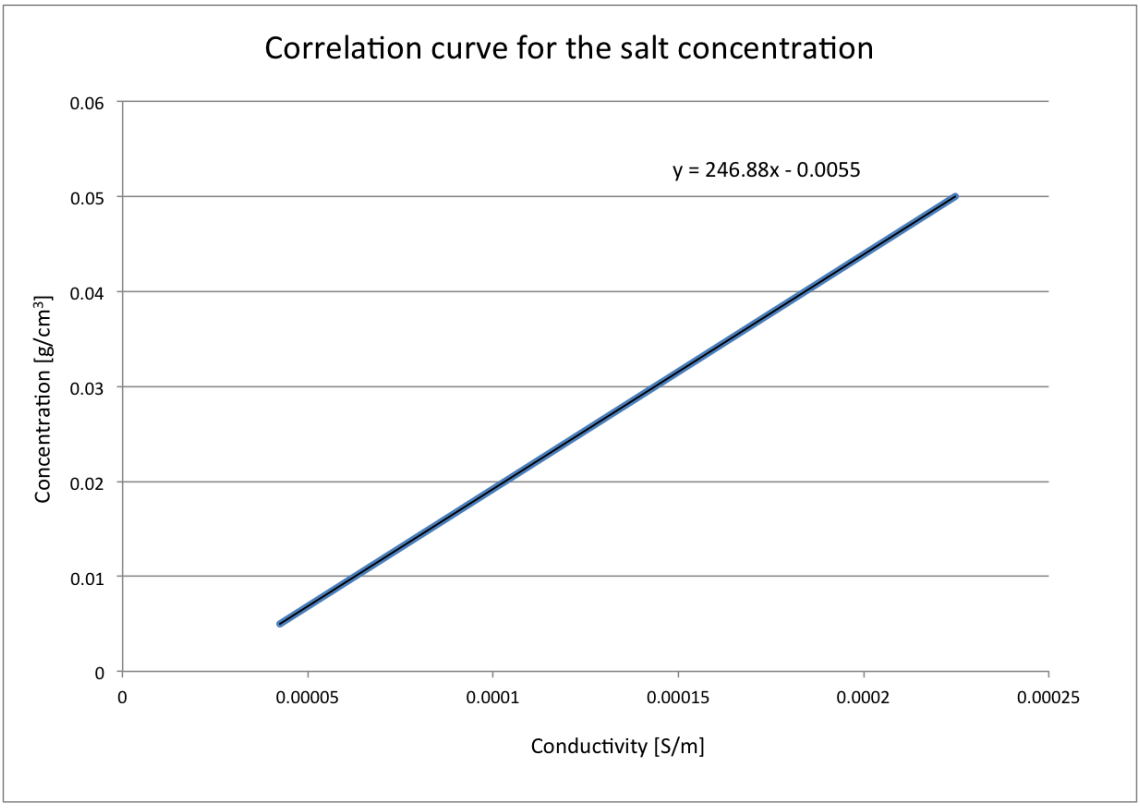

Figure 4.4: Correlation curve for the *NaCl* concentration.

The *NaCl* over the core can be found by using the linear Equation 4.4.

$$y = 246.88x - 0.0055 \tag{4.4}$$

Where y is the concentration in g/cm^3 and x is the measured conductance.

When the resistivity apparatus output is constant over a long enough period of time,

the experiment is done. The resistivity data have to be processed by calculating the conductivity and the concentration versus time over the core sample.

Chapter 5

Matlab Implementation

In one dimension the diffusion Equation is simplified to:

$$\frac{\partial c}{\partial t} = D\frac{\partial^2 c}{\partial x^2} \tag{5.1}$$

Where $c(x,t)$ is the unknown function to be solved for, x as a coordinate in space and t as coordinate in time. D is the diffusion coefficient which determines how fast c changes in time. Since the experiment is done in a porous media this equation has to include the porosity and formation factor, since there are only the pores that are available for diffusion. So Equation 2.10 from Chapter 2.1.2 has to be solved numerically

$$\frac{\partial c}{\partial t} = \frac{D}{\phi F}\frac{\partial^2 c}{\partial c^2}$$

This implementation of the diffusion equation is solved by using the Crank Nicolson method, which is a numerical solution where there is applied centered differences in both space and time [32].

Before the equation can be solved numerically, the boundary and initial conditions has to be defined, to obtain a unique solution. To define these conditions the Dirichlet and Neumann conditions are used. The Dirichlet boundary condition specify requirements for the concentration on the boundary. While the Neumann condition impose the flux of concentration though the top and the bottom [9].

In the Crank Nicolson solution centered differences in both space and time are applied, combined with an average in time. This demand the PDE to be fulfilled at the spatial mesh points, but in between the points in the time mesh:

$$\frac{\partial}{\partial t}c(x_i,t_{n+\frac{1}{2}}) = \frac{D}{\phi F}\frac{\partial^2}{\partial x^2}c(x_i,t_{n+\frac{1}{2}})$$

for $i = 1,...,N_{x-1}$ and $n = 0,...,N_{t-1}$. On the right hand side we get the expression:

$$\frac{1}{\Delta x^2}(c_{i-1}^{n+\frac{1}{2}} - 2c_i^{n+\frac{1}{2}} + c_{i+1}^{n+\frac{1}{2}})$$

Estimate the term $c_i^{n+\frac{1}{2}}$ by an arithmetic average:

$$c_i^{n+\frac{1}{2}} \approx \frac{1}{2}(c_i^n + c_i^{n+1})$$

Then we get this expression:

$$-\frac{D}{2\Delta x^2}c_{i-1}^{n+1} + (\frac{1}{\Delta t} + \frac{D}{\Delta x^2})c_i^{n+1} - \frac{D}{2\Delta x^2}c_{i+1}^{n+1} = \frac{D}{2\Delta x^2}c_{i-1}^{n} + (\frac{1}{\Delta t} - \frac{D}{\Delta x^2})c_i^{n} + \frac{D}{2\Delta x^2}c_{i+1}^{n} \tag{5.2}$$

After multiplying Equation 5.2 with Δt and $r = \frac{D\Delta t}{\phi F 2\Delta x^2}$ the following expression is derived.

$$-rc_{i+1}^{n+1} + (1+2r)c_i^{n+1} - rc_{i-1}^{n+1} = rc_{i+1}^{n} + (1-2r)c_i^{n} + rc_{i-1}^{n} \tag{5.3}$$

Equation 5.3 is a tridiagonal problem, so u_i^{n+1} may be efficiently solved by using the tridiagonal matrix algorithm; $Au^{n+1} = Bu^n$. Matrix A and B and the two vectors u^{n+1} and u^n are stated under.

$$u^{n+1} = \begin{bmatrix} u_0^{n+1} \\ \vdots \\ u_i^{n+1} \end{bmatrix}$$

$$A = \begin{bmatrix} (1+2r) & -r & 0 & \cdots & 0 \\ -r & (1+2r) & -r & \cdots & 0 \\ 0 & \ddots & \ddots & \ddots & 0 \\ 0 & \cdots & -r & (1+2r) & -r \\ 0 & 0 & \cdots & -r & (1+2r) \end{bmatrix}$$

$$B = \begin{bmatrix} (1-2r) & r & 0 & \cdots & 0 \\ r & (1-2r) & r & \cdots & 0 \\ 0 & \ddots & \ddots & \ddots & 0 \\ 0 & \cdots & r & (1-2r) & r \\ 0 & 0 & \cdots & r & (1-2r) \end{bmatrix}$$

$$u^n = \begin{bmatrix} u_0^n \\ \vdots \\ u_i^n \end{bmatrix}$$

5.1 Unsteady State Solution

For the unsteady state numerical solution the concentration under the core is constant, but the concentration over the core will increase with time. So the Dirichlet boundary condition will correspond to the constant concentration under the core, and Neumann to the concentration flux over the core. When the Neumann and the Dirichlet boundary conditions are applied to this tridiagonal problem, we get that u_1^n is equal to C_{bottom} and u_i^n is equal to $C_{top}(n-1)$. To run this numerical simulation the matrices have to be symmetrical, and we can see from the matrices A and B that the first and last line make the matrices non-symmetrical. So two vectors which includes these boundaries are used, all the values will be zero except for the first and the last value. So by using the first and last line in $Au^{n+1} = Bu^n$ the two boundary vectors are expressed as:

$$b = \begin{bmatrix} -rC_{bottom} \\ 0 \\ \vdots \\ -rC_{n-1} \end{bmatrix} \quad \text{and} \quad k = \begin{bmatrix} rC_{bottom} \\ 0 \\ \vdots \\ rC_{n-1} \end{bmatrix}$$

The final expression for u^{n+1} is then

$$u^{n+1} = Bu^n A^{-1} + (k-b) \tag{5.4}$$

The matlab code for the unsteady state simulation can be found in Appendix C, and the algorithm is presented on the next page.

Algorithm 1 The Crank-Nicolson Method for Unsteady State Diffusion

Require: $D, Q, C_{bottom}, C_{top}, Lx, nx, totalTime, nt, \phi$

Set

$dx = \frac{L_x}{nx}$

$dt = \frac{totalTime}{nt}$

$D_e = DQ$

Crank Nicolson Scheme

$-rc_{i+1}^{t+1} + (1+2r)c_i^{t+1} - rc_{i-1}^{t+1} = rc_{i+1}^{t} + (1-2r)c_i^{t} + rc_{i-1}^{t}$

$r = \frac{D_e dt}{2\phi dx^2}$

Populate sparse matrices for time step t and $t+1$ from dx to L_x, stepsize dx to form tridiagonal matrices along band -1 to 1

$-rc_{i+1}^{t+1} + (1+2r)c_i^{t+1} - rc_{i-1}^{t+1}$

$rc_{i+1}^{t} + (1-2r)c_i^{t} + rc_{i-1}^{t}$

$i = 1, 2, 3..., nx$

Set Neumann conditions

Set Dirichlet conditions

for $t = 2, .., nt$

Solve matrix equation using the Conjugate Gradient Method

Store concentration data for timestep t

Create surface plot

end for

5.1.1 The Conjugate Gradient Method

To solve the tridiagonal matrices problem the conjugate gradient method is used. The conjugate gradient method is an algorithm for the numerical solution of a system of linear equations, in this case for matrices that are symmetric and positive-definite. The method of Conjugate Gradients is an iterative method, which seeks for a minimum of a function [33]. The equation that needs to be solved with the conjugate gradient method is:

$$Au^{n+1} = Bu^n \tag{5.5}$$

Where A is a known $n \times n$ matrix, and Bu^n is a known $n \times 1$ vector and u^{n+1} is an $n \times 1$ vector of unknowns. To find u^{n+1} the conjugate gradient method is efficient to use [34]. The matlab code for the conjugate gradient method is presented in Appendix C and the algorithm for this method is presented on the next page.

Algorithm 2 The Conjugate Gradient Method

Require: A, b, x_0, e, N

$r_0 = b - Ax_0$

$p_0 = 0$

$\alpha_0 = 0$

$w_0 = 0$

for $m = 1, ..., N$ **do**

$x_m = x_{m-1} + \alpha_{m-1} p_{m-1}$

$r_m = r_{m-1} - \alpha_{m-1} p_{m-1}$

if $||r_m|| < e$ **then**

return x_m and m.

end if

$\beta_m = (r_m^T r_m)/(r_{m-1}^T r_{m-1})$

$p_m = r_m + \beta_m p_{m-1}$

$w_m = A p_m$

$\alpha_m = (r_m^T r_m)/(p_m^T w_m)$

end for

return Message: "CG did not converge within the maximum number of iterations.", x^{m+1} and m.

5.1.2 Validation of the Unsteady State Code

To validate the unsteady state numerical solution, it was run with boundary conditions that apply for a steady state solution. For a steady state solution the concentration at both sides of the core will be constant during the whole experiment. So the Dirichlet boundary condition will correspond to the constant concentrations at the top and at the bottom of the core. While the Neumann condition will be the constant flux in the whole core. Thus the only thing that has to be changed is the boundary conditions for the concentration on the top of the core. The vectors b and k represent the boundary conditions, so by changing $b(nx,1)$ to the constant $-rC_{top}$ and $k(nx,1)$ to the constant rC_{top}, the simulation should stabilize at a linear relationship between time and concentration and the flux should be constant. The matlab code for this is found in Appendix C.

Chapter 6

Results and Evaluation

In this Chapter the results from the experimental preparations, the main experiment and the numerical simulations are presented.

6.1 Experimental Preparations Results

The relevant core plug data are shown in Table 6.1. Two core plugs of different length was used in this thesis, core plug A and core plug B. The reason for this was because it was impossible to measure the resistivity over the core plug A with the laboratory resistivity apparatus, core plug A was also to small to get an accurate enough reading from the Helium Porosimeter. Thus core plug B was also needed for measurements of the porosity.

Table 6.1: Core plugs data.

Core	**Length**(*mm*)	**Diameter**(*mm*)
Core plug A	6.12	37.12
Core plug B	40.00	37.08

The porosity of the core plugs was found by measuring the porosity of core plug B. If core plug A had been put in the Helium Porosimeter, there would be a lot of uncertainties because the core holder is fitted for a core plug of approximately 40 mm. The core plugs

was thoroughly cleaned and dried, so the results from the Helium Porosimeter should be accurate and reliable. The data obtained from the Helium Porosimeter experiment is shown in Table 6.2. The porosity for the core sample was calculated by using Equation 3.4 and 3.5, and is denoted by ϕ in Table 6.2.

Table 6.2: Data from the Helium Porosimeter measurements.

V_1 (cm^3)	$V_2(cm^3)$	$V_m(cm^3)$	$V_b(cm^3)$	ϕ
50.5	17.3	33.2	43.169	0.231

The resistivity over the core plugs were only measured for the core sample B. The distance between the electrodes in the resistivity apparatus was to long for the core plug A. One has to take the core plug out of the saltwater to measure the resistivity over the core, this can increase the resistivity measurement remarkable, because the saltwater will starts to evaporate at once it is taken out of the water. The data presented in Table 6.3 is from the resistivity apparatus measurements. From these data the resistivity for the rock fully saturated with brine, with 5 wt% $NaCl$, was obtained by using Equation 2.17. In Table 6.4 R_w and R_o from four measurements are shown, and the calculated formation factor. The resistivity apparatus is sensitive, and the formation factor is an important parameter for this thesis, therefore this experiment was preformed four times.

Table 6.3: Results of the resistivity measurements

U_r (V)	$U_x(V)$	$r_r(\Omega)$	$r_x(\Omega)$
2.190	0.597	1000	272.600
2.770	0.436	1000	157.400
2.830	0.425	1000	150.176
2.790	0.431	1000	154.480

6.2 Results From the Diffusion Experiment

The raw data, the resistivity data, for the unsteady state experiments are shown in Figure 6.1. The same experiment was preformed four times, but with different core samples.

Table 6.4: Data used to calculate the formation factor and the calculated formation factor.

R_o (Ωm)	$R_w(\Omega m)$	$Formation factor$
7.25	0.15	48.33
4.25	0.15	28.33
4.05	0.15	27.03
4.17	0.15	27.80

All the core plugs were from the same core that had been cut into several cores of smaller lengths. The four cores were all 6 mm long, and all had the same diameter, which is stated in Table 6.1 under core plug A.

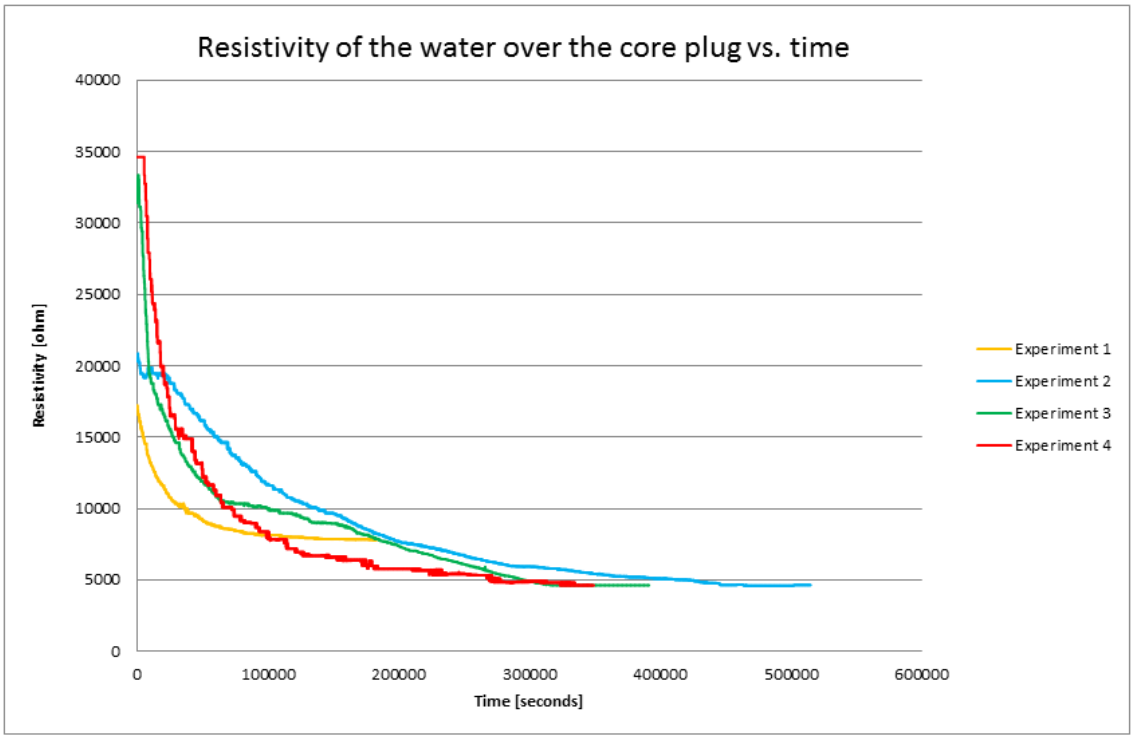

Figure 6.1: Resistivity in the water over the core sample for all the experiments.

Parameters from the experiments which are important for the numerical simulations are collected in Table 6.5. For each experiment the volume over the core, denoted V in Table 6.5, will change a little, the same yields for the salt concentration in the distilled water above the core before the experiment starts, C_0. The salt concentration in the water above the core before start is assumed to be equal to the first reading of the resistivity. The end concentration of salt in the water volume above the core is also individual for each

experiment, it is denoted C_e in Table 6.5. The salt concentration in the tank, C_s, is the same for all of the experiments.

Table 6.5: Data from the experiments.

Parameter	**Ex. 1**	**Ex.2**	**Ex. 3**	**Ex. 4**
$V[cm^3]$	22	20	18	20
$C_0[g/cm^3]$	0.0088	0.0066	0.002	0.0016
$C_s[g/cm^3]$	0.05	0.05	0.05	0.05
$C_e[g/cm^3]$	0.0262	0.0477	0.0478	0.0479
$\Delta t[sec]$	183 000	514 800	392 300	349 200

6.3 Validation of the Numerical Unsteady State Solution

As a validation of the unsteady state numerical solution, it was tested that it converged to the steady state solution, how this is done is described in Chapter 5.1.2. The numerical simulation results with fixed concentration at both ends, in other words a steady state, are presented in Figure 6.2, 6.3 and 6.4. The results shows that the numerical simulation for an unsteady state experiment also work for steady state conditions.

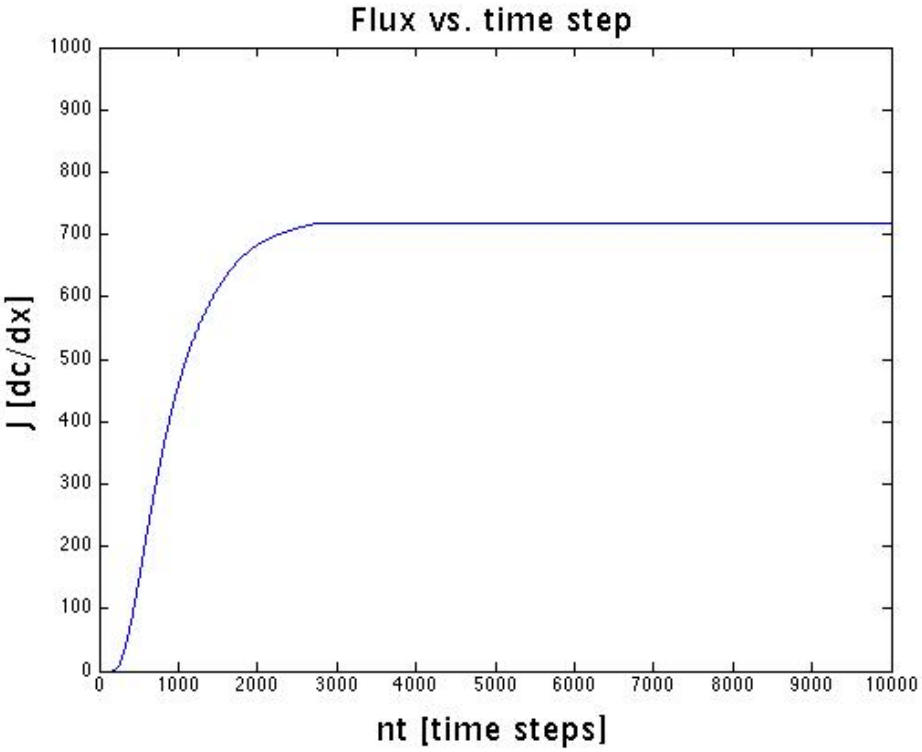

Figure 6.2: The flux stabilizes, which indicates a converge to a steady state solution.

When the flux is constant, the numerical simulation have reach a steady state. Can see from Figure 6.2 that the flux stabilizes around 700, this validates that the numerical solution converges to a steady state solution. When the diffusion simulation reach steady state there should be a linear relationship between the concentration and the time, as in Figure 6.4. The linear relationship shown in Figure 6.4 correspond to the end result (the top) in Figure 6.3.

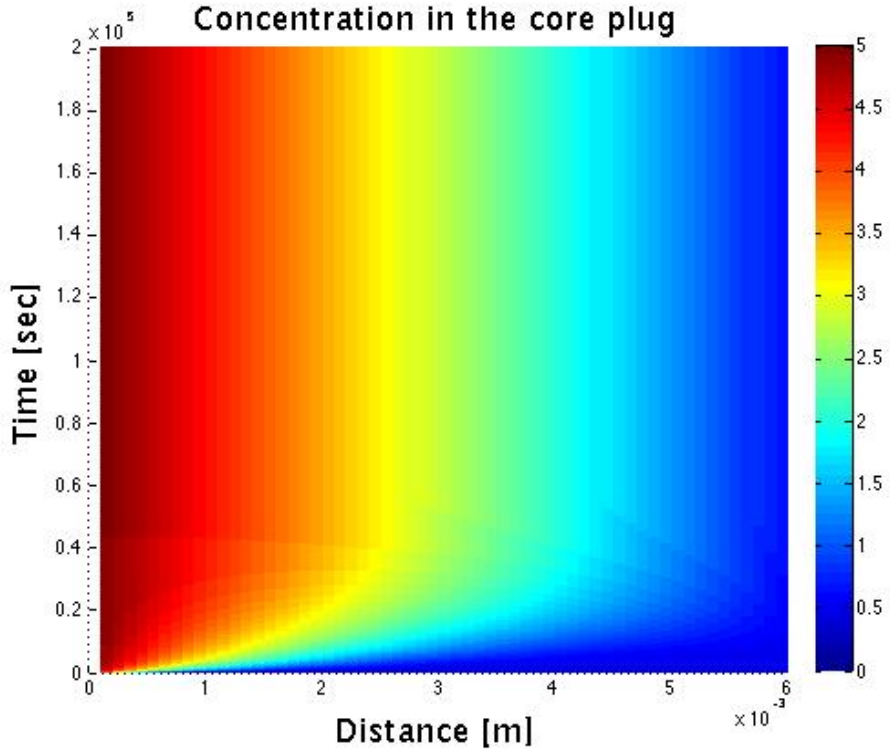

Figure 6.3: The concentration in the core when a steady state simulation is preformed.

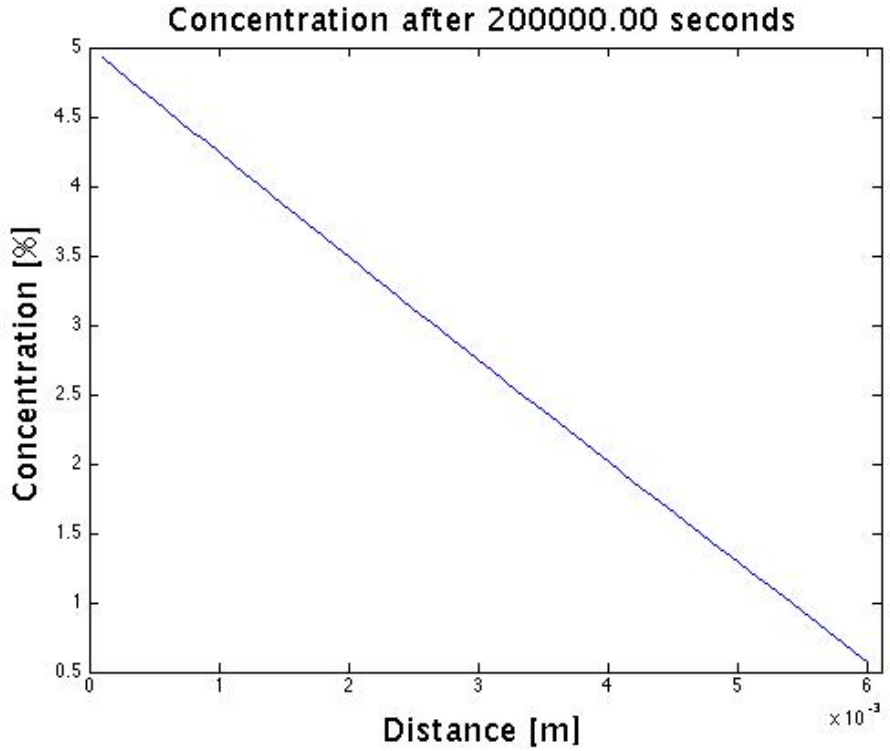

Figure 6.4: The concentration in the core after the simulation is done.

6.4 Evaluation of the Diffusibility

A steady state experiment could be more optimal for estimation for the effective diffusion coefficient. Unfortunately we lacked the necessary equipment to conduct such an experiment. So the most accurate effective diffusion coefficient is found by match the plotted experimental resistivity and concentration curves, with the numerical simulation curves simulated with different diffusivbility values (Q). For every simulation the concentration in the water over the core was stored for each time step, and imported to excel. Then the concentration data was converted to conductivity and resistivity, and plotted into the plot with the experimental data. The $\frac{1}{Q}$ range was run between 10 and 40. There are two parameters that have to be changed in the numerical code for each experiment, the volume of the water over the core and the concentration of salt in this volume (before start), both parameters are found in Table 6.5.

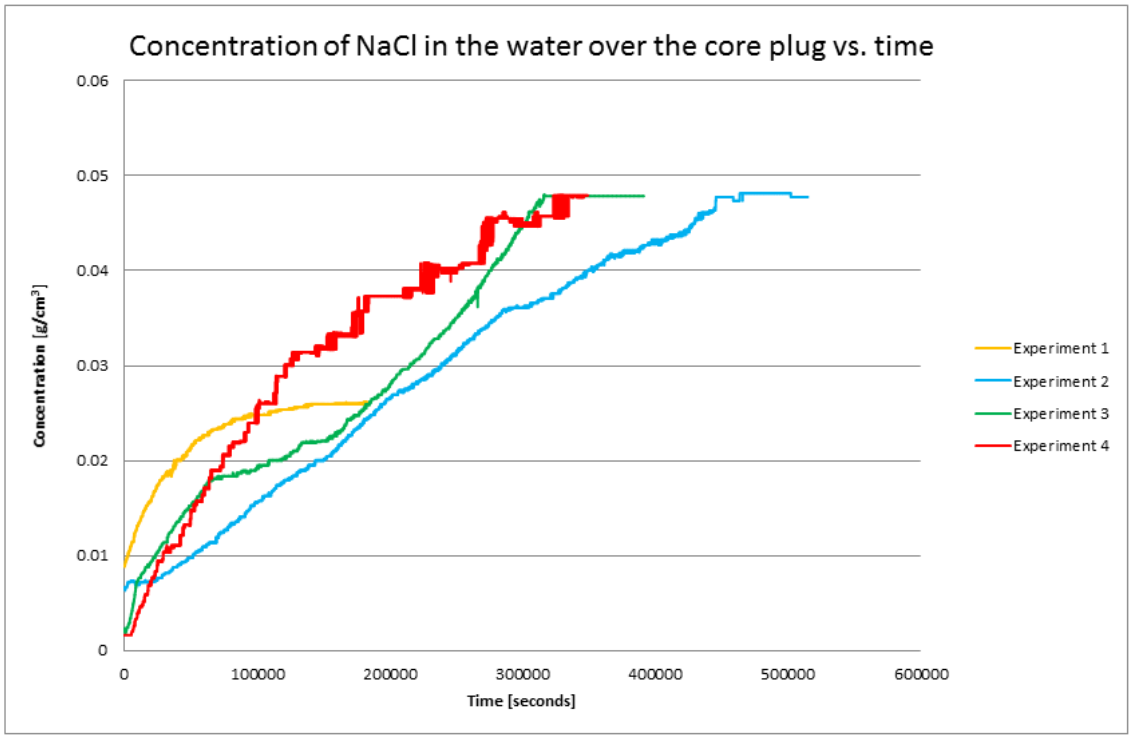

Figure 6.5: The concentration of NaCl above the core sample from all of the experiments.

To do this matching the raw data from the experiments has to be converted first to the conductivity of the water and then to the concentration, by using the correlation described in Chapter 4.2 and Equation 4.4. In Figure 6.5 the concentration of *NaCl* in the water over

the core sample is plotted against time for all of the experiments. Experiment two to four stabilizes at almost the same concentration, while the end concentration for experiment one stabilizes at an unexpectedly low value. Most likely something has gone wrong during the preparations of the experiment or during the experiment.

Then the numerical simulation has to be run for the different diffusibility values. This was done again for each experiment, because of the slightly different input parameters, V and C_0. The plotted result, both resistivity and concentration, from the simulations with different values of Q, is presented in Figure 6.6 and 6.7.

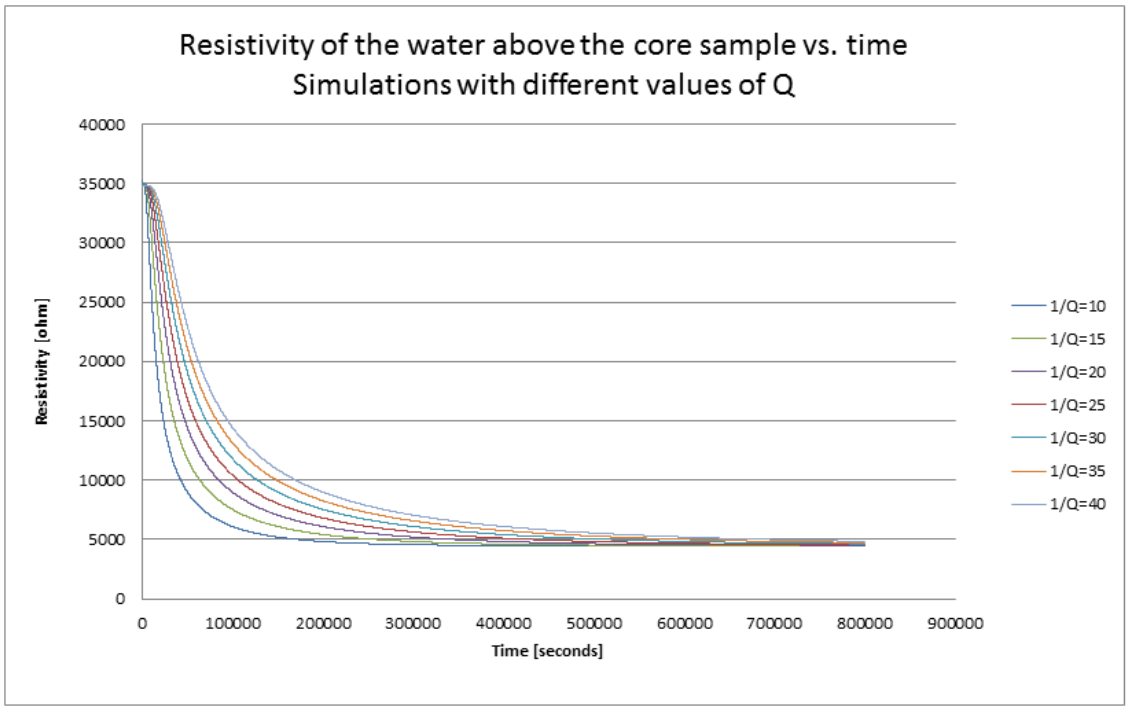

Figure 6.6: The plotted simulated resistivity for different Q values.

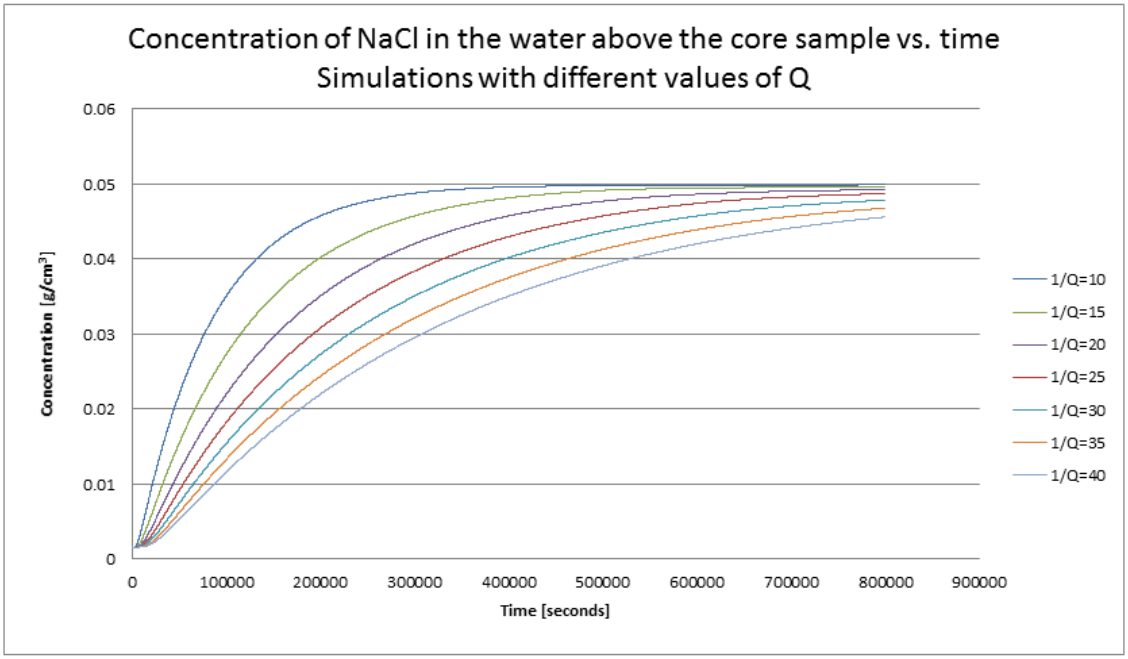

Figure 6.7: The plotted simulated concentration for different Q values..

Chapter 7

Discussion

Since the parameters have been measured in the laboratory, there will always be different sources of error. Especially since there was a need to use a core plug of a longer length to measure the formation factor and porosity, than the ones used in the diffusion experiment.

7.1 Porosity

The porosity for core plug B was found to be around 23.1 %. Since all of the cores used in this thesis was from the same original core sample, the porosities are assumed to be almost the same value. However porosities variations can be local, exemplary a small layer of clay or shale will reduce the porosity dramatically for a core sample with a length of only 6 mm. So most likely the porosities does vary between the cores used in this thesis, the results from the diffusion experiment indicate that the core sample is much more heterogeneous than expected. The porosity for the Berea sandstone usually lays between 13 % - 23% [27], so the sample used in this thesis is in the high end, but still within the expected range.

7.2 Formation Factor

There were done four experiments to measure the formation factor, due to the first one was unexpectedly high. The first formation factor measured was so much higher than the rest because the core was most likely not fully saturated with saltwater, which will increase the resistivity of the core and consequently increase the formation factor. When using the resistivity measurement apparatus in the laboratory one has to take the core out of the saltwater. When the core sample is taken out of the brine the resistivity will increase quickly, because the water will immediately starts to evaporate. So to get the correct value for the resistivity for a 100% saturated core, the measurement has to be done as quick as possible. The first measured value was neglected when the average formation factor was calculated. The average formation factor was estimated to be 27.72, which is assumed to be too high. The R_w value was also just estimated, and not measured in the lab, because the lab did not have any apparatus to measure the resistivity in water.

7.3 Estimation of the Diffusibility from the Experimental and Numerical Data

Experiment One

The resistivity curve and the concentration curve for experiment one together with the numerical simulations are shown in Figure 7.1 and 7.2. The thick pink line represents the experimental data.

It is not possible to conclude with anything from the experimental data for experiment one, the experimental curve is not even close to any of the plotted simulated values. At the start of the diffusion process experiment one look like a good match for the simulated curve with a diffusibility value of $1/10$, but then something happens (around 10 hours into the experiment). Something probably have gone wrong around this point, but it is difficult to know what the cause is.

There can be many reasons why this experiment failed, it may be the core sample, it can

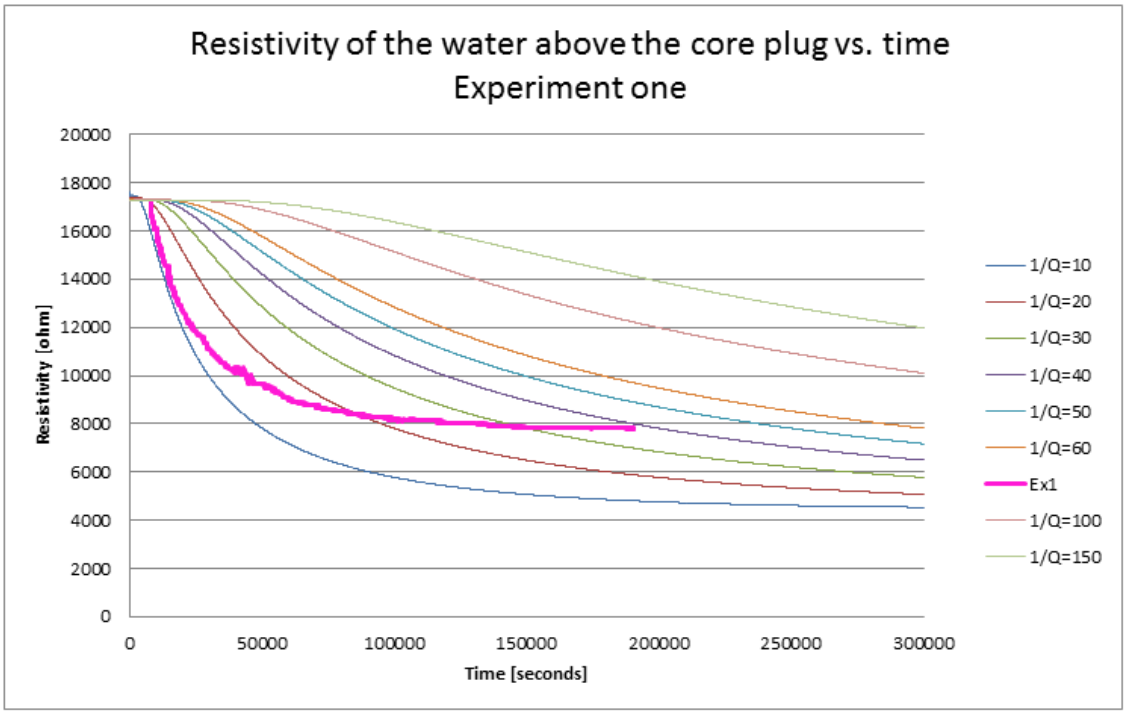

Figure 7.1: Resistivity in the water over the above core, experiment one and data from matlab simulations with different values of the diffusibility.

be a human error or just bad readings/connections. As mentioned earlier the same core plug was never used twice, maybe this specific core plug had a layer of clay, which makes it almost impermeable or reduces the porosity dramatically. It can have been an error with the two electrodes, which were taped to the inside of the core-sleeve. The tape that was used to do this was just a regular tape, and not water resistant. So the tape may have loosen when it was in the water long enough, and one of the electrodes may have slipped under the tape. There was nothing to cover the tank with, so dust and other dirt particles have most likely fell into the brine during the experiment. Maybe one of the dust/dirt particles started to diffuse through the core, and then got stuck, and ended up blocking the way for the salt ions. This is very unlikely, but it can have happened. Since this was the first time this experiment was preformed there was no indication of how long the diffusion would take. The experiment was stopped when the resistivity readings was constant over a longer period. The concentration of $NaCl$ in the water over the core may have started to increase again, if we just had waited longer.

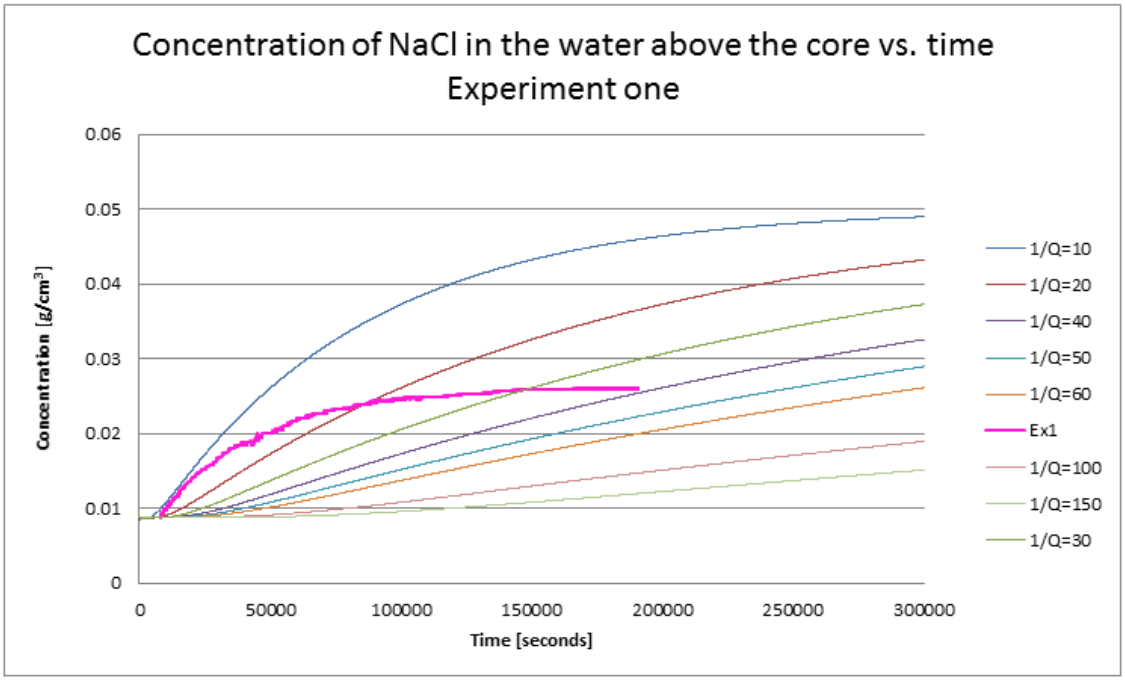

Figure 7.2: Concentration of *NaCl* in the water volume over the core, for experiment one and matlab simulations.

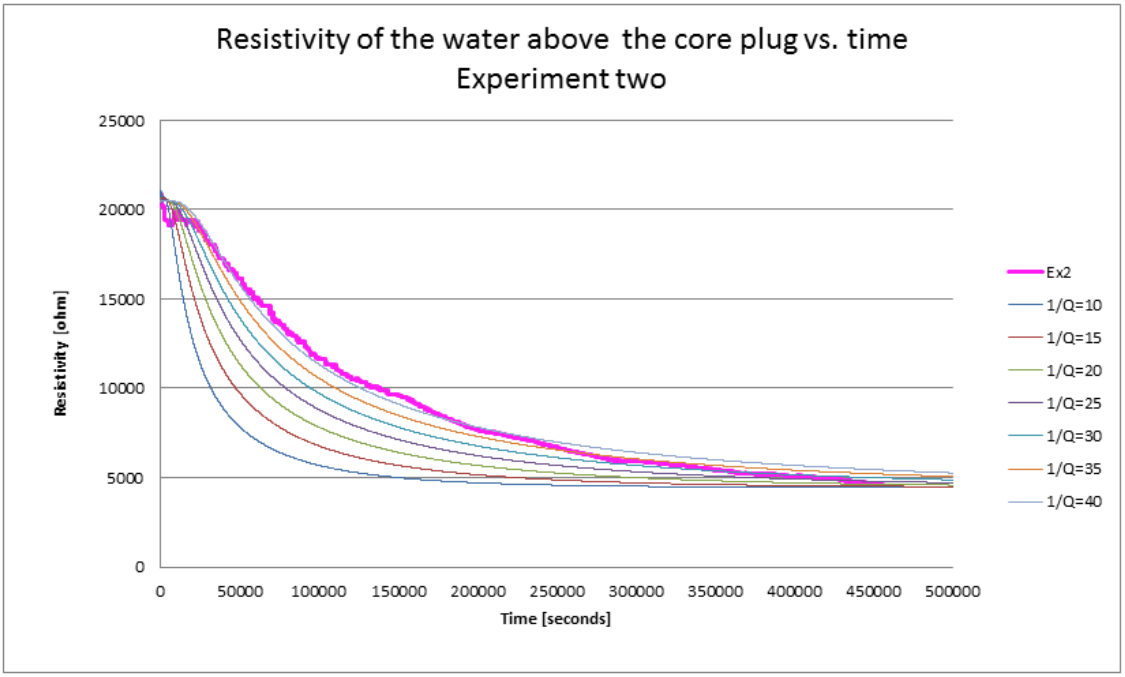

Figure 7.3: Resistivity of the water over the core plug, experiment two and matlab simulations with different diffusibility values.

Experiment Two

The results from experiment two are presented in Figure 7.3 and 7.4, together with the

simulated data for different values of Q. This experimental curve is a much better fit with the simulated curves, than the plotted data from experiment one. For the first halftime, until around 65 hours into the experiment, the experimental data line lays around the line that are plotted for a $1/Q$ of 40, and then the concentration increases rapidly for a while, and ends up at the line which is plotted for a $1/Q$ of 20. Thus the inverse diffusibility for the core sample used in experiment two may lay in between 20 and 40.

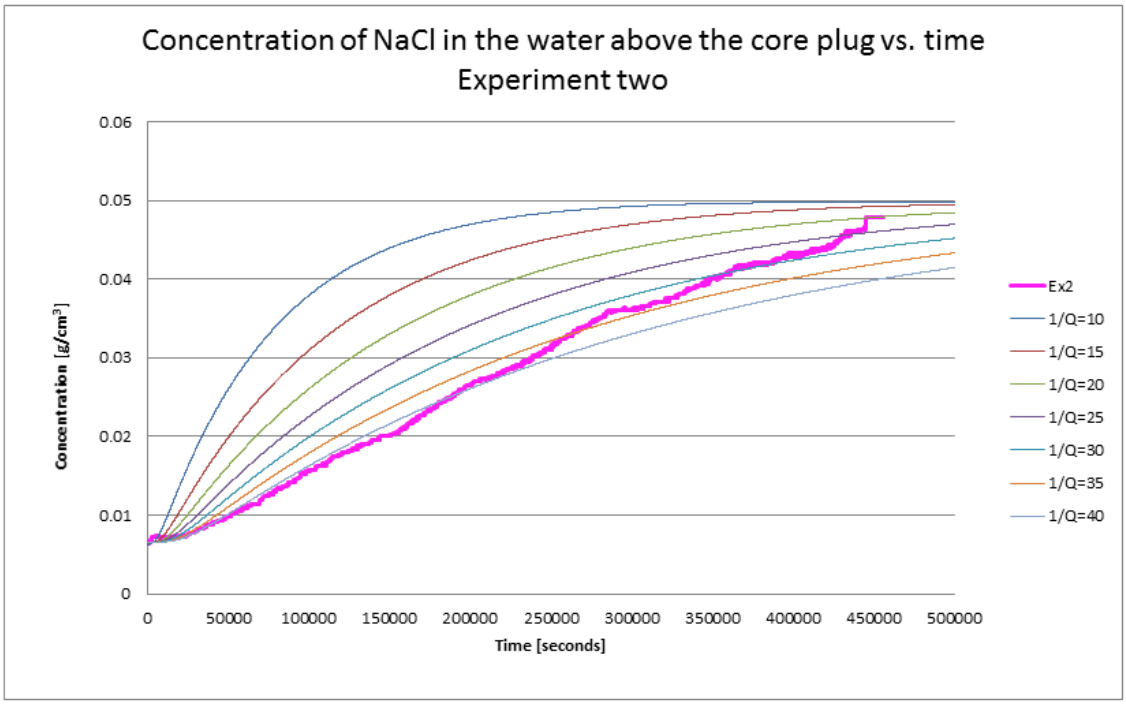

Figure 7.4: Concentration of *NaCl* in the water above the core, experiment two and different numerical simulations.

Experiment Three

The experimental plotted data and the simulated plotted data for experiment three are shown in Figure 7.5 and 7.6. From the resistivity curve and concentration curve one can conclude that something have slowed down the diffusion process, after approximately 18 hours. The experimental plotted data both start and end around the curve for a $1/Q$ between 10 and 15, when the diffusion process is slower the curve lays between a $1/Q$ of respectively 25 and 30. There is no obvious reasons of why the diffusion suddenly slowed down in the middle of the experiment. The tank can have been moved, which would stir up the saltwater and this would most likely have an influence on the diffusion through the core. Or maybe someone have poured tap water or distilled water into the tank, but that is

very doubtful.

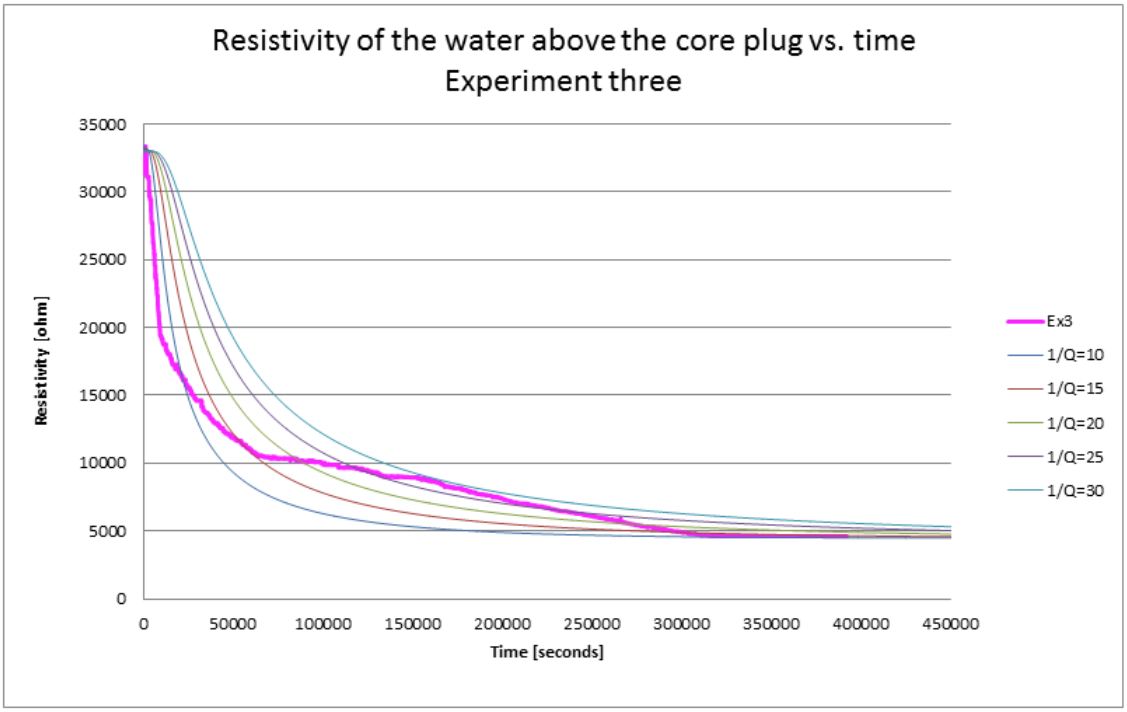

Figure 7.5: Resistivity of the water above the core plug, experiment three and from matlab simulations with different Q values.

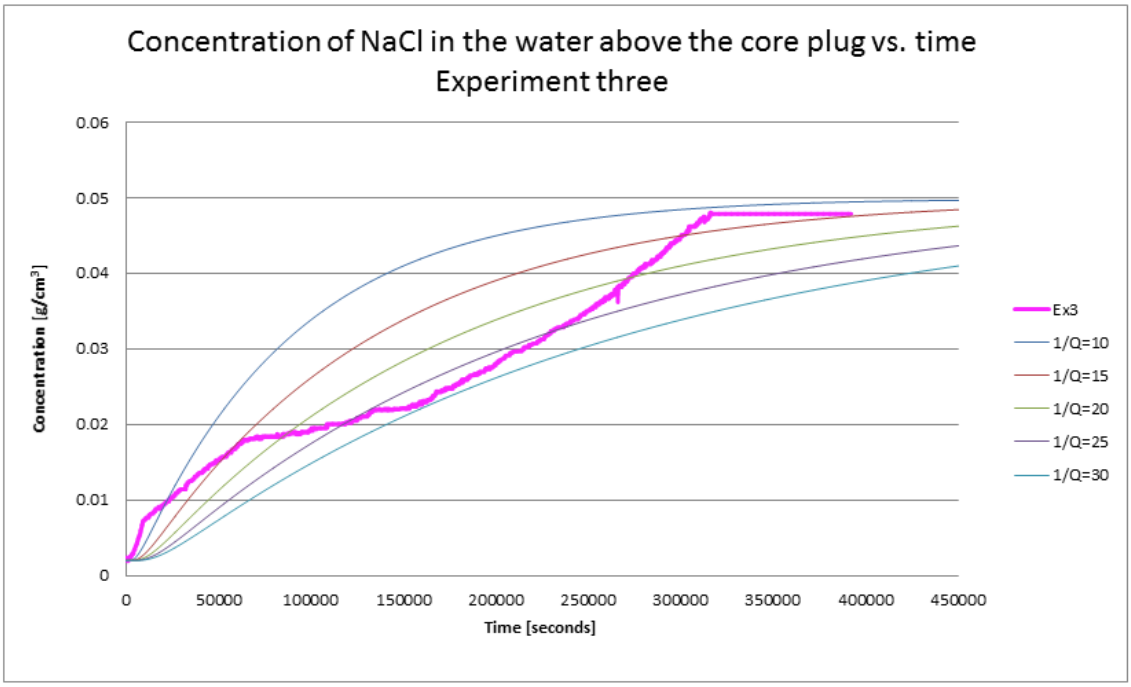

Figure 7.6: Concentration of *NaCl* in the water above the core plug, experiment three and simulated data.

Experiment Four

This is the experiment with the best fit together with experiment two, when compared to the simulated results. Figure 7.7 and 7.8 shows the resistivity curve and concentration curve for experiment four and the simulated data for experiment four. The curve from experiment four lays between the simulated curves with the $1/Q$ value of 15 and 20, during the entire experiment time.

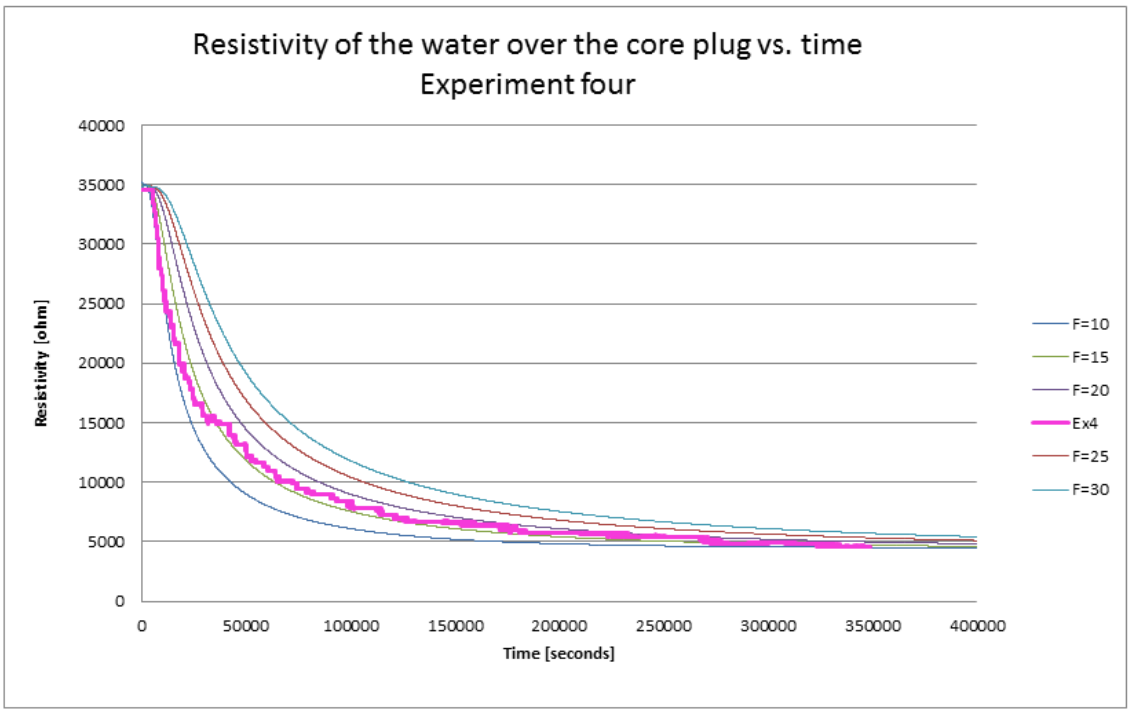

Figure 7.7: Resistivity in the water above the core plug, experiment four and from the numerical simulations.

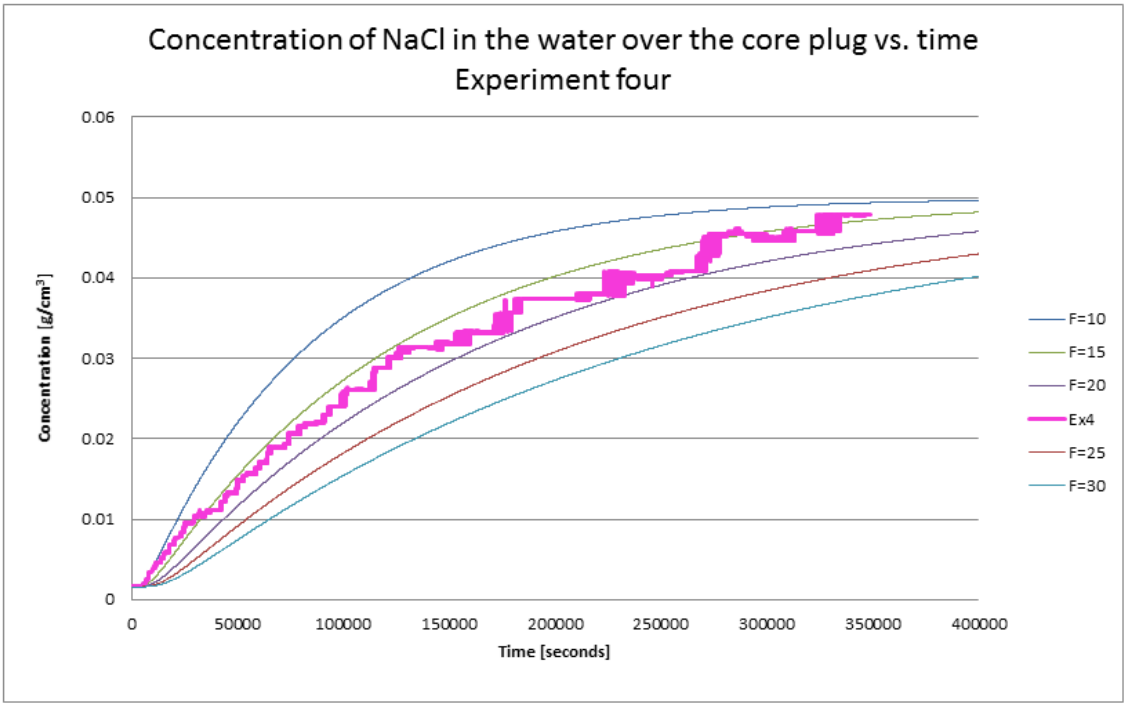

Figure 7.8: Concentration of *NaCl* in the water over the core plug, experiment four and simulated data.

7.4 The Effective Diffusion Coefficient and Formation Factor

When the diffusibility values are estimated it is possible to calculate the effective diffusion coefficient by using Equation 2.9, the diffusion coefficient for *NaCl* in water is $2 \times 10^{-5} cm^2/sec$.

$$D_e = DQ$$

The formation factors from the diffusion experiments can then be estimated. The effective diffusion coefficients and formation factors are presented in Table 7.1. It was not calculated from experiment one, because it was not possible to get a good estimation of the diffusibility. Since all of the core plugs are from the same core sample the remarkable variation of

Table 7.1: Formation factor and the effective diffusion coefficient from experiment two to four.

Parameter	**Ex. two**	**Ex. three**	**Ex. four**
$D_e\ [cm^2/sec]$	6.66×10^{-7}	1×10^{-6}	1.17×10^{-6}
F	30	20	17

the estimated formation factors are unexpected. Experiment two and four gave the most reliable curves, but also very different formation factor values. This indicate that the core sample used in this thesis may have been more heterogeneous than a typically Berea sandstone core sample.

If a core sample is heterogeneous there is a lot of local variations of the rock properties, like porosity and permeability. So as discussed under experiment one, the four different core plugs can have different clay content, porosities and permeabilities. All of which will have an effect on the diffusion process and the estimated effective diffusion coefficient and the diffusibility.

The measured formation factor from the laboratory resistivity apparatus was 27.72, and from the experiment the formation factor lays between 17 and 30. The formation factor calculated from the resistivity measurements was expected to be lower than the formation factors estimated from the experiments. The reason why this was not the case, may be because the resistivity apparatus in the laboratory may not be in the best shape. It would also have been a more accurate resistivity measure if there was possible to have the core plug in the brine when the resistance was measured. Some of the saltwater most likely evaporate at once the core is taken out of the water, which will increase the resistivity over the core and increase the formation factor. If there had been possible to measure the R_w value in the laboratory, this would also have given a more accurate formation factor.

When there is clay minerals present in the sandstone, it will increase the conductivity, there will be more ways for the ions to pass than just trough the pore space. There is no such thing that can increase the diffusion, since this can only happen in the pore space. Therefore a lower formation factor from the resistivity measurements was predicted, unfortunately this was not the results for this thesis, unless one only look at the results from experiment two and the calculated formation factor. If we compare the estimated formation factor from experiment two, which was 30, with the calculated formation factor, 27.72, we got an expected result. However since the estimated formation factors was so different, unfortunately one can not conclude with anything even if experiment two is a good match.

Core plug B may contain very small amount of clay particles since the formation factor calculated from the resistivity measurements was remarkable high, so little that the clay did not decrease the resistivity over the core. Since the formation factor estimated from the diffusion experiment varies between 17 and 30, this may indicate that the core sample used in this thesis is more heterogeneous than a regular Berea sandstone core sample. So the core sample may contain remarkable small amounts of clay minerals compared to the regular Berea sandstone, but be remarkable more heterogeneous than the regular Berea sandstone.

Clay content in formations will obviously affect the resistivity logs, by decreasing the readings, when downhole logging is preformed. The resistivity logs are often used to confirm that there are hydrocarbon present in the formation, though hydrocarbons will give a high resistivity reading. So a reliable evaluation of the clay content is essential in formation evaluation.

The purpose with this thesis was to try to prove that the formation factor calculated from resistivity measurement was lower than the formation factor estimated from diffusion. If this had been the case one could have concluded further with that the Berea sandstone actually contain severals percent of clay minerals, and further on how important it is with a reliable evaluation of the clay content when doing an evaluation of different formations and that the clay actual have a remarkable impact on the resistivity measurements.

There are several different sources of error in this thesis, and it may be therefore the expected results was not achieved. Unfortunately there was not enough time to try to get this fixed. The formation factor calculated from the resistivity over the core, was done on a different core plug than the ones were the diffusion was measured. The same yield for the porosity measurement, it was only done for core plug B. Another error can be that the electrodes was a little bit over the top of the core sample, 2-5 mm, and the $NaCl$ ions will use a little bit longer time to reach the electrodes than they use to reach the top of the core sample.

If there had been time, we should have done the diffusion experiment on the same core plug several times, and also measured the formation factor and porosity of this core plug. Since the core plug need to be saturated with distilled water before the experiment,

and after the experiment it is most likely saturated with the brine, the core plug would have to be cleaned and dried before it can be used for the experiment one more time. Unfortunately it was not enough time to do this.

Chapter 8

Conclusion

- There is clearly an analogy between the diffusion and the electrical conductivity in porous media. Both describes the movement of a substance down a concentration gradient and both is dependent on the pore geometry and porosity.
- The effect of clay content in formations have an impact on the resistivity measurements, which is often used to estimate hydrocarbon bearing zones. Therefor it is important to have good estimate of the clay content in the different formations.
- The Berea sandstone usually contains between zero and 15 % of clay minerals.
- The average formation factor calculated from resistivity measurement was estimated to be 27.72.
- The same unsteady state experiment was preformed four times in this thesis, where one of them was discharged as an out lier. The rest of them gave fair results, and there was possible to estimate the diffusibility for each experiment by comparing the experimental data to the simulated data with different diffusibility values. Then the formation factors was estimated to be; 30, 20 and 17.
- The numerically simulation was a good fit with the experimental data, especially for experiment two and four. Which indicates that the numerical code was accurate enough.
- The remarkable change in the formation factor for the diffusion experiment may

indicate that the core sample used for this thesis is more heterogeneous than expected.

- It was expected that the formation factor calculated from the resistivity measurements should be lower than the formation factor values estimated from the diffusion experiments. This was expected because when there is clay minerals present in the sandstone, the conductivity will increase, because there will be more "ways" for the electrical charged ions to pass through than just the pore space of the rock. In case of a diffusion, the molecules only can pass through the pore space.
- The purpose with this thesis was to try to show that the formation factor calculated from resistivity measurement was lower than the formation factor estimated from diffusion. Unfortunately this was not the case. If it had been the case one could have concluded further with how important it is with a reliable evaluation of the clay content when doing evaluation of different formations and that the clay actual have an impact on the resistivity measurements.
- There may have been too many sources of error for this experiment, all of the experiments and measurements should have been preformed on the same core plug.

8.1 Further work

- Preform the steady state experiment with a pump that work at the low pump rate which this experiment require. Then it will be easier to estimate the effective diffusion coefficient and the formation factor.
- Do both the unsteady state and steady state experiment several times with the same core.
- Do a more accurate resistivity measurement over the core and of the saltwater to improve the formation factor calculations. It is also essential to do the resistivity measurement over the core plug A, the core plug used in the diffusion experiment, the same yields for the porosity measurement.

Nomenclature

ϕ	Porosity
σ_o	Conductance of the fully saturated rock
σ_w	Conductance to the solution
τ	Tortuosity
A	Cross sectional area of the core sample $[m^2]$
C	Concentration $[mol/m^3]$
C_0	The concentration of salt in the water above the core, before the start of the experiment.
C_e	The concentration of salt in the water above the core at the end of the experiment.
C_s	The concentration of salt in the saltwater.
D	Diffusion coefficient/diffusitivity $[m^2/s]$
D_e	Effective diffusion $[m^2/sec]$
F	Formation factor
I	Current
J	Diffusion flux $[kg/m^2sec]$
J_x	Diffusion flux in x-direction $[molm^{-2}s^{-1}]$
L	Length of the core sample $[m]$
m	Cementation exponent

P	Pressure
Q	Diffusibility
R_0	Resistivity of fully saturated rock [*ohmm*]
R_w	Resistivity to the solution [*ohmm*]
t	Time [seconds]
U	Voltage
V	Volume of distilled water above the core.
V	Volume
V_b	The cores bulk volume
V_m	The matrix volume
x	Position, length

References

[1] Iguchi M. and Ilegbusi O. *Basic Transport Phenomena in Materials Engineering*. chapter 8: Diffusion and Mass Transfer, pages: 135-147. 2014.

[2] Klinkenberg L. J. "Analogy Between Diffusion and Electrical Conductivity in Porous Rocks." *Bulletin of the Geological Society of America* (1951).

[3] PERM inc. *Fundamentals of Fluid Flow in Porous Media, Chapter two Formation Resistivity Factor*. URL: http://perminc.com/resources/fundamentals-of-fluid-flow-in-porous-media/chapter-2-the-porous-medium/formation-resistivity-factor/.

[4] Paul A., Laurila T., Vuorinen V., and Divinski S. *Thermodynamics, Diffusion and the Kirkendall Effect in Solids*. chapter 3: Fick's Laws of Diffusion, pages: 115-139. 2014.

[5] Nakashima Y. and Nakano T. "Accuracy of formation factors for three-dimensional pore-scale images of geo-materials estimated by renormalization technique." *Journal of Applied Geophysics 75, 31-41* (2011).

[6] Ellis W. and Singer J. *Well Logging for Earth Scientists*. Chapter: Clay Quantification pages: 597-627. 1987.

[7] Perkins T. and Johnston O. "A Review of Diffusion and Dispersion in Porous Media". *SPE 480* (1963).

[8] Suni I. *Introduction to Materials Science and Engineering*. Chapter 6: Diffusion. 2012.

[9] Mehrer H. *Diffusion in Solids*. pages: 26-313. 2007.

[10] Roth K. *Soil Physics*. pages: 31-74. 2012.

[11] Taheri S., Abedi J, and Kantzas A. “Prediction of Effective Diffusion and Dispersion Coefficients, Considering Different Flow and Heterogeneity Properties of Porous Media.” *SPE 165520* (2013).

[12] Aronofsky J. and Heller J. “A Diffusion Model to Explain Mixing of Flowing Miscible Fluids in Porous Media”. *SPE 860-G* (1957).

[13] Fondriest Environmental. *Conductivity, Salinity and Total Dissolved Solids.* URL: `http://www.fondriest.com/environmental-measurements/parameters/water-quality/conductivity-salinity-tds/`.

[14] Torsæter O. and Abtahi M. “Experimental Reservoir Engineering, Laboratory Workbook”. *Department of Petroleum Engineering and Applied Geophysics, The Norwegian University of Science and Technology* (2003).

[15] Archie G. E. “The Electrical Resistivity Log as an Aid in Determining Some Reservoir Characteristics”. *Dallas Meeting* (1941).

[16] Garboczi E., Bentz D., Snyder K., Martys N., Stutzman P., Ferraris C., and Bullard J. *The relationship between the formation factor and the diffusion coefficient of porous materials saturated with concentrated electrolytes: Theoretical and experimental considerations*. URL: `https://ciks.cbt.nist.gov/~garbocz/FFvDiff/FFvDiff/node1.html`.

[17] Schlueter E., Myer L., Cook N., and Witherspoon P. “Formation Factor and the Microscopic Distribution of Wetting Phase in Pore Space of Berea Sandstone”. *Lawrence Berkeley Laboratory - 33207* (1992).

[18] Devarajan S., Torres-Verdin C., and Thomas E. “Pore-Scale Analysis of The Waxman-Smits Shaly Sand Conductivity Model”. *Annual Logging Symposium* (2006).

[19] Zhan X., Schwartz L., Toksoz M., SMith W., and Morgan F. “Pore-Scale modeling of Electrical and Fluid Transport in Berea Sandstone”. *Geophysics, Vol 75, No. 5* (2010).

[20] Dullien F.A.L. *Porous Media: Fluid Transport and Pore Structure*. pages: 306-313. 1992.

[21] Berg C. F. “Re-Examining Archie’s Law: Conductance Description by Tortuosity and Constriction”. *Physical Review E 86, 046314* (2012).

[22] Schlumberger. *Oilfield Glossary: Tortuosity*. URL: http://www.glossary.oilfield.slb.com/Terms/t/tortuosity.aspx.

[23] U.S. Environmental Protection Agency - Environmental Geophysics. *Factors Influencing Electrical Conductivity*. URL: https://archive.epa.gov/esd/archive-geophysics/web/html/factors_influencing_electrical_conductivity.html.

[24] Wenzheng Y., Guo T., Xiyuan C., Hongxiu J., and Hongwu M. "Investigation of Effects of Clay content on F-Phi Relationship by Lattic Gas Automation Using Digital Rock Model". *China University of Petroleum* (2011).

[25] Poupon A. and Gaymard R. "The Evaluation of Clay Content From Logs". *SPWLA Eleventh Annual Logging Symposium* (1970).

[26] Glover P. *Clay Effects on Porosity and Resistivity Logs*. pages: 270-282. 2012.

[27] Berea Sandstone TM. *Berea Sandstone TM Petroleum Cores*. URL: http://www.bereasandstonecores.com/.

[28] Dahab A., Omar A., Sayyouh M., and Hemeida A. "Effects of Clay Content on Permeability Damage, Capillary Pressure and Wettability Characteristics of Saudi Reservoir Rocks." *Petroleum Dept., King Saud University, Saudi Arabia* (1992).

[29] Dvorkin J. and Nur A. "Scale of Experiment an Rock Physics Trends". *Stanford University, Special Section: Rock Physics* (2009).

[30] Oleoresins. *Principle of Soxhlet Extraction and Experimental Setup of Soxhlet Extractor*. URL: http://oleoresins.melbia.com/principle-of-soxhlet-extraction-and-experimental-setup.html.

[31] Nasa. *Glenn Research Center: Boyle's Law*. URL: https://www.grc.nasa.gov/www/k-12/airplane/boyle.html.

[32] Crank J. *The Mathematics of Diffusion*. pages: 144-148. 1975.

[33] Shewchuk J. "An Introduction to the Conjugate Gradient Method Without the Agonizing Pain". *School of Computer Science, Carnegie Mellon University* (1994).

[34] Albl C. "Conjugate Gradients Explained". *Department of Cybernetics, Czech Technical University in Prague* (2012).

Appendices

Appendix A

Analytical Solution to Fick's Second law

$$\phi \frac{\partial C}{\partial t} = D_e \frac{\partial^2 C}{\partial x^2} \tag{A.1}$$

$D_e/\phi = D^*$ is a constant, use the function $y = f(x,t)$ defined by

$$y = \frac{x}{2\sqrt{D^* t}} \tag{A.2}$$

The partial derivatives of equation A.2 are

$$\frac{\partial y}{\partial x} = \frac{1}{2\sqrt{D^* t}} \qquad \text{and} \qquad \frac{\partial y}{\partial t} = -\frac{x}{4\sqrt{D^* t^3}} \tag{A.3}$$

By definition

$$\frac{\partial C}{\partial t} = \frac{dC}{dy}\frac{\partial y}{\partial t} = -\frac{x}{4\sqrt{D^* t^3}}\frac{dC}{dy} \tag{A.4}$$

and

$$\frac{\partial^2 C}{\partial x^2} = \frac{\partial}{\partial x}[\frac{dC}{dy}(\frac{\partial y}{\partial x})] = \frac{1}{4D^* t}\frac{d^2 C}{dy^2} \tag{A.5}$$

Substituting equation A.4 and A.5 into equation A.1 yields

$$\frac{dC}{dy} = -\frac{\sqrt{D^* T}}{x}\frac{d^2 C}{dy^2} \tag{A.6}$$

Combining equation A.2 and A.6 gives

$$\frac{dC}{dy} = -\frac{1}{2y}\frac{d^2C}{dy^2} \tag{A.7}$$

Set $z = dC/dy$, and we get this expression to solve:

$$z = -\frac{1}{2y}\frac{dz}{dy} \tag{A.8}$$

Which is an integral

$$-2\int ydy = \int \frac{dz}{z} \tag{A.9}$$

with the solution

$$-y^2 = lnz - lnA \tag{A.10}$$

Where A is an integration constant. By rearranging the solution, we get this expression for z:

$$z = Aexp(-y^2) \tag{A.11}$$

and

$$\int dC = A\int exp(-y^2)dy \tag{A.12}$$

The solution of the integrals in equation A.12 are based on a set of boundary conditions. So these have to be set:

For $t = 0$, $C_x = C_0$ at $0 < y < \infty$

For $t = 0$, $C = C_s$, the constant concentration at $y = 0$

$C = C_s$ at $y = \infty$

$$\int_{C_0}^{C_x} dC = A\int_0^y exp(-y^2)dy \tag{A.13}$$

And the solution to the integral in equation A.13 yields:

$$C_x - C_0 = \frac{2}{\sqrt{\pi}}(C_s - C_0)\frac{\sqrt{\pi}}{2}erf(y) \tag{A.14}$$

$$\frac{C_x - C_0}{C_s - C_0} = erf(\frac{x}{2\sqrt{D^*t}}) \tag{A.15}$$

Appendix B

Resistivity for NaCl Solutions

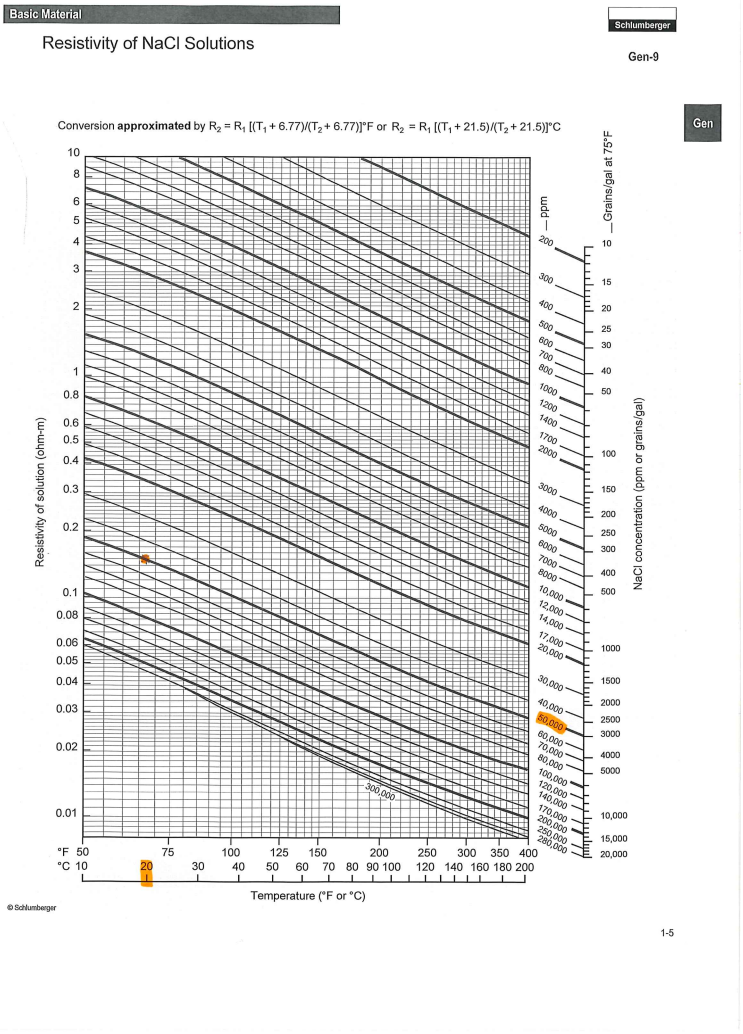

Appendix C

Matlab Codes

Numerical Crank Nicolson - Steady State

```
clear all
close all
%Define the constants, diffc= Diffusion coefficient
%for NaCl in water at 20
%degrees celsius. a = the effectiv diffusion
%coefficient, calculated from
%the formation factor and the diffusion coefficient.
diffc=2e-9; %diffusion coefficient NaCl e-9 m2/s
phi=0.231; %porosity of the core sample
F = 48.327; %formation factor of the core sample
a = diffc/F;  %a= effective diffusion coefficient,
%assumed: a = diffc/F
Cbot = 5; %weight precent of salt at the bottom of the core
Ctop = 0.5; %approximated weight precent of salt at
%the top of the core

%defining lenght of reservoir, maximum runtime # of
%nodes and corresponding
```

```
%intervals
Lx = 0.006; %meter
nx = 60; %number of space steps
dx = Lx/nx; %width of space steps
X = (dx:dx:Lx);

totalTime = 466650; %Total time in seconds
nt        = 10000; %number of time steps
dt        = totalTime/nt; %wifth of time steps
T = (0.5*dt:dt:totalTime-0.5*dt);

r =a*dt/(2*(dx^2)*phi); %constant

%populating matrix to fit system of equations
%defined by At1*pt1 = At0*p0
%[A]1 corresponds to solution matrix (timestep 't+1')
%[A]0 corresponds to matrix for known values (timestep 't')
%dirichlet and neumann boundary applied directly
%into solution matrix

e         = ones(nx,1);
At1       = spdiags([(-r*e) (1+2*r)*e (-r*e)],-1:1,nx,nx);
%sparse matrix defining differentials for t = n+1
pt1       = (ones(nx,1));
% vector to be solved specifying pressure for t = n+1
At0       = spdiags([r*e (1-2*r)*e r*e], -1:1,nx,nx);
pt0       = (Ctop*ones(nx,1));

Imax = 10;
pMatrix = zeros(nx,Imax); %solution matrix, where
%all the solution vectors are stored as the loop run
```

```
50 err = 1e-4;
51
52 c = At0*pt0;
53 %c=pt0;
54
55 %Specify the boundary conditions
56 b = zeros(nx,1);
57 b(1,1) = -Cbot*r;
58 b(nx,1) = -Ctop*r;
59 k = zeros(nx,1);
60 k(1,1) = Cbot*r;
61 k(nx,1) = Ctop*r;
62
63 graduOutletM = zeros(nt,1);
64 timesM = zeros(nt,1);
65
66 for t = 2:nt
67
68      %solving px for timestep t+1
69       pt1 = CG(At1,c,pt1,err,Imax);
70
71
72     %storing concentration data for time t
73      pMatrix(:,t) = pt1 ;
74     %updating solution vector
75      c = At0*pt1 +(k-b)  ;
76     %pMatrix(:,t) = c;
77
78     %plotting %'concentrationfor time step t-1'
79     %capturing each 10th plot frame
80      if mod(t,10) == 0
```

```
81              figure(1)
82              plot(X,pMatrix(:,t))
83              ylim([Ctop,Cbot]);
84              xlim([0,Lx+dx]);
85              xlabel('Distance [m]','FontSize',18,'FontName',
86              'Computer Modern');
87              ylabel('Concentration [%]','FontSize',18,'FontName',
88              'Computer Modern');
89              title(sprintf('Concentration after %8.2f
90              seconds', t*dt),
91              'FontSize',18,'FontName','Computer Modern');
92             M(t/1)= getframe(gcf);
93
94          end
95
96          graduOutletM(t)=(pMatrix(nx,t)-0.5)/dx;
97          times(t)=t;
98
99      end
100     pMatrix;
101     figure(2)
102     plot(times,graduOutletM)
103     ylim([0,1000]);
104     ylabel('J [dc/dx]','FontSize',18,'FontName','Computer Modern');
105     xlabel('nt [time steps]','FontSize',18,'FontName',
106     'Computer Modern');
107
108     [H,K]=meshgrid(T,X);
109
110     figure(3)
111     surf(K,H,pMatrix,'EdgeColor','none');
```

```
112 ylabel('xTime [sec]','FontSize',18,'FontName',
113 'Computer Modern');
114 xlabel('yDistance [m]','FontSize',18,'FontName',
115 'Computer Modern');
116 zlabel('Concentration[%]','FontSize',18,'FontName','
117 Computer Modern');
118 title(sprintf('Concentration after %8.2f seconds',
119 t*dt),'FontSize',18,'FontName','Computer Modern');
120 colorbar
121 caxis([0 5]);
```

Numerical Crank Nicolson - Unsteady State

```
clear all
close all
%Define the constants, diffc= Diffusion coefficient
%for NaCl in water at 20
%degrees celsius. a = the effectiv diffusion
%coefficient, calculated from
%the formation factor, porosity and the diffusion
%coefficient.
diffc=2e-9; %diffusion coefficient NaCl e-9 m2/s cm2/s
phi=0.231; %porosity of the core sample
F = 20; %formation factor of the core sample. F for
%the different experiments:
%Ex1: F=150, Ex2: F=33, Ex3 and Ex4: F=31
a = diffc/F;  %a= effective diffusion coefficient,
%assumed: a = diffc/F
Cbot = 5; %weight precent of salt at the bottom of the
%core g/cm3
Ctop = 0.2; %approximated weight precent of salt at
%the top of the core at start g/cm3
%For different experiments: Ex1: Ctop=0.88, Ex2:
%Ctop=0.66, Ex3: Ctop=0.2,
%Ex4: Ctop=0.16
V = 2e-5; %volume over the core m^3 L V= 20, ex1 ex4,
%22 ex3, 18 ex2
A = 1.082e-3; % area core m^2

%defining lenght of reservoir, maximum runtime # of
%nodes and corresponding
%intervals
```

```
30 Lx = 0.006; %meter
31 nx = 100; %number of space steps
32 dx = Lx/nx; %width of space steps
33 X = (dx:dx:Lx);
34
35 totalTime = 400000; %Total time in seconds
36 nt        = 20000; %number of time steps
37 dt        = totalTime/nt; %wifth of time steps
38 T         =(0.5*dt:dt:totalTime-0.5*dt);
39
40 r =a*dt/(2*(dx^2)*phi); %constant
41
42 %populating matrix to fit system of equations defined
43 %by At1*pt1 = At0*p0
44 %[A]1 corresponds to solution matrix (timestep 't+1')
45 %[A]0 corresponds to matrix for known values
46 %(timestep 't')
47 %dirichlet and neumann boundary applied directly into
48 %solution matrix
49
50 e         = ones(nx,1);
51 At1       = spdiags([(-r*e) (1+2*r)*e (-r*e)],-1:1,nx,nx);
52 %sparse
53 %matrix defining differentials for t = n+1
54 pt1       = (ones(nx,1));% vector to be solved
55 %specifying pressure for t = n+1
56 At0       = spdiags([r*e (1-2*r)*e r*e], -1:1,nx,nx);
57 pt0       = (Ctop*ones(nx,1));
58
59 Imax = 10;
60 pMatrix = zeros(nx,Imax); %solution matrix, where all
```

```
61 %the solution vectors are stored as the loop run
62 err = 1e-4;
63
64 c = At0*pt0;
65
66 graduOutletM = zeros(nt,1);
67 timesM = zeros(nt,1);
68 Vconc = zeros(nt,1);
69 ConcVolume = zeros(nt,1);%vector with all the
70 %concentrations over the core
71 ub=Ctop;
72 for t = 2:nt
73
74     b = zeros(nx,1);
75     b(1,1) = -r*Cbot;
76     b(nx,1) = -(r*ub);
77     k = zeros(nx,1);
78     k(1,1) = r*Cbot;
79     k(nx,1) = r*ub;
80
81      %solving px for timestep t+1
82      pt1 = CG(At1,c,pt1,err,Imax);
83
84     %printing desired time values
85     %storing concentration data for time t
86     %updating solution vector
87
88     c = At0*pt1 + (k-b);
89
90     %updating the boundary conditions
91     gradc=(c(nx-1)-ub)/dx;
```

```
92      flux=(gradc*a*A)/phi;  %area and porosity
93      Massin=flux*dt;
94      MassV=Massin+ub*V;
95      ub=MassV/V;
96
97      %storing concentration data for time t
98      pMatrix(:,t) = pt1;
99
100     graduOutletM(t)=(pMatrix(nx,t)-pMatrix(nx,t-1))/dx;
101     times(t)=t;
102     Vconc (t) = ub;
103
104     %plotting %'concentration across reservoir for
105     %time step t-1'
106     %capturing each 10th plot frame
107
108    if mod(t,10) == 0
109         figure(1)
110         plot(X,pMatrix(:,t))
111         ylim([Ctop,Cbot]);
112         xlim([0,Lx+dx]);
113         xlabel('Distance [m]','FontSize',18,'FontName',
114         'Computer Modern');
115        ylabel('Concentration [%]','FontSize',18,'FontName',
116        'Computer Modern');
117        title(sprintf('Concentration after %8.2f seconds',
118        t*dt),
119        'FontSize',18,'FontName','Computer Modern');
120       M(t/1)= getframe(gcf);
121     end
122 end
```

```
123 pMatrix;
124 figure(2)
125 plot(times,graduOutletM) %plots the flux vs. time
126 ylim([0,50]);
127
128 [H,K]=meshgrid(T,X);
129
130 figure(4)
131 surf(K,H,pMatrix,'EdgeColor','none');
132       ylabel('Time [sec]','FontSize',18,'FontName',
133       'Computer Modern');
134       xlabel('Distance [m]','FontSize',18,'FontName',
135       'Computer Modern');
136       zlabel('Concentration','FontSize',18,'FontName',
137       'Computer Modern');
138       title(sprintf('Concentration after %8.2f seconds',
139       t*dt),
140       'FontSize',18,'FontName','Computer Modern');
141       colorbar
142       caxis([0 5]);
```

The Conjugate Gradient Method

```
function [xM, m] = CG(A,b,x0,err,N)
%implementation of the Conjugate Gradient method
%[hereafter denoted 'CG']
%CG numerically computes solution of matrix equation by
%approximating the
%solution which minimizes the gradient of f =
%0.5*x'*A*x - x'*b
% which is also the solution to A*x = b

%A = matrix equation
%b = solution vector
%x0 = guess at x-vector to be solved
%rM0 = residual at step m-1
%rM = residual at step m (stop criteria vs. error tolerance)
%pM = conjugate direction
%alphaM = weight of pM0 in computation of xM
%betaM = weight of pM0 in computation of pM
%wM = A*pM computed for next time step

%assigning input to initial residual
rM0 = b-A*x0;
pM = 0;
alphaM = 0;
wM = 0;

for i = 1:N

    %computing approximation of x and residual at step m
    xM = x0+alphaM*pM;
```

```
30      rM = rM0-alphaM*wM;
31      %stop criterion applied such that every single
32      %index of vector
33      %has to fulfill the given error tolerance
34      if sum(abs(rM) > err) == 0
35          m = i;
36          return
37      end
38      %assigning values to variables for step m+1
39      betaM   = (rM'*rM)/(rM0'*rM0);
40      pM      = rM+betaM*pM;
41      wM      = A*pM;
42      alphaM  = (rM'*rM)/(pM'*wM);
43      rM0     = rM;
44      x0      = xM;
45  end
46
47  disp('CG did not converge within the maximum iterations!')
48
49  end
```

Appendix D

Additional Results from Experiments

In this appendix additional results from the experiments is presented.

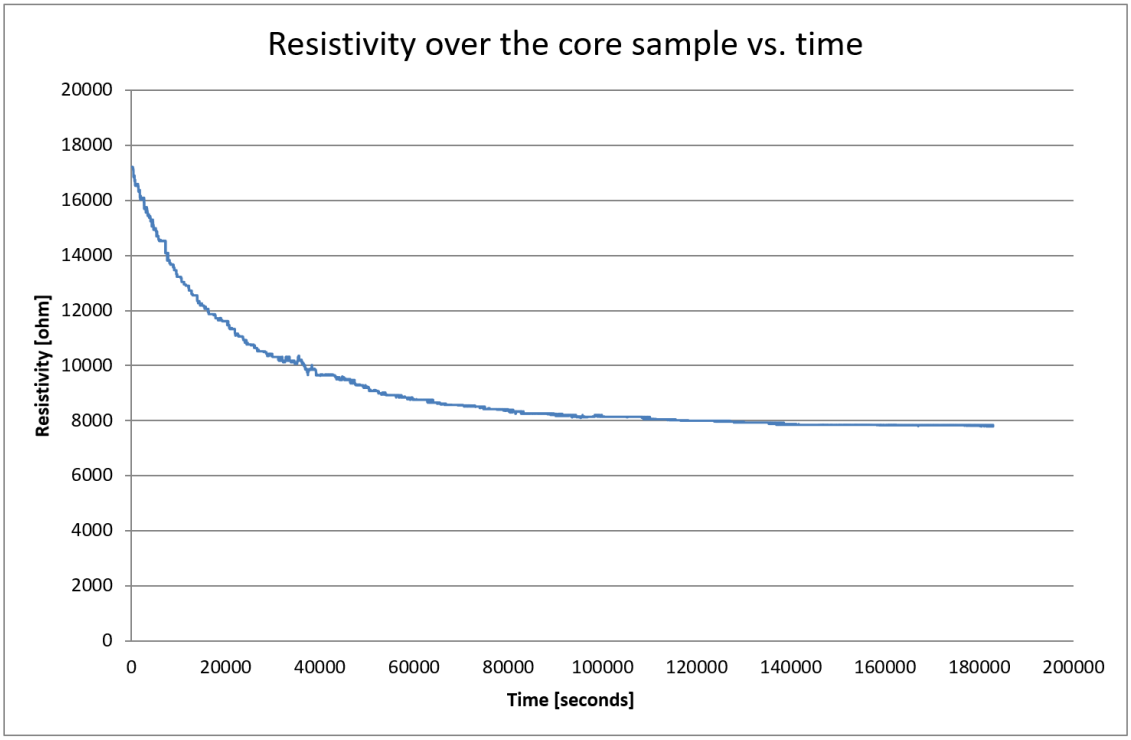

Figure D.1: Resistivity in the water over the core plug, Experiment one.

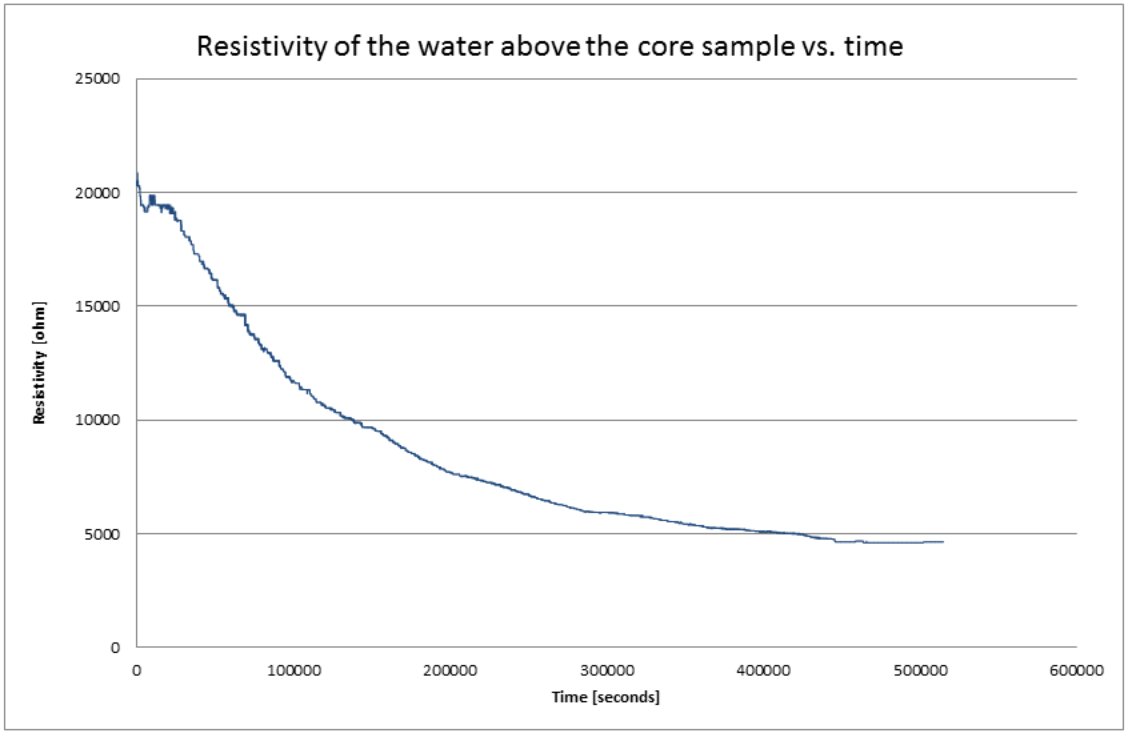

Figure D.2: Resistivity in the water over the core plug, Experiment two.

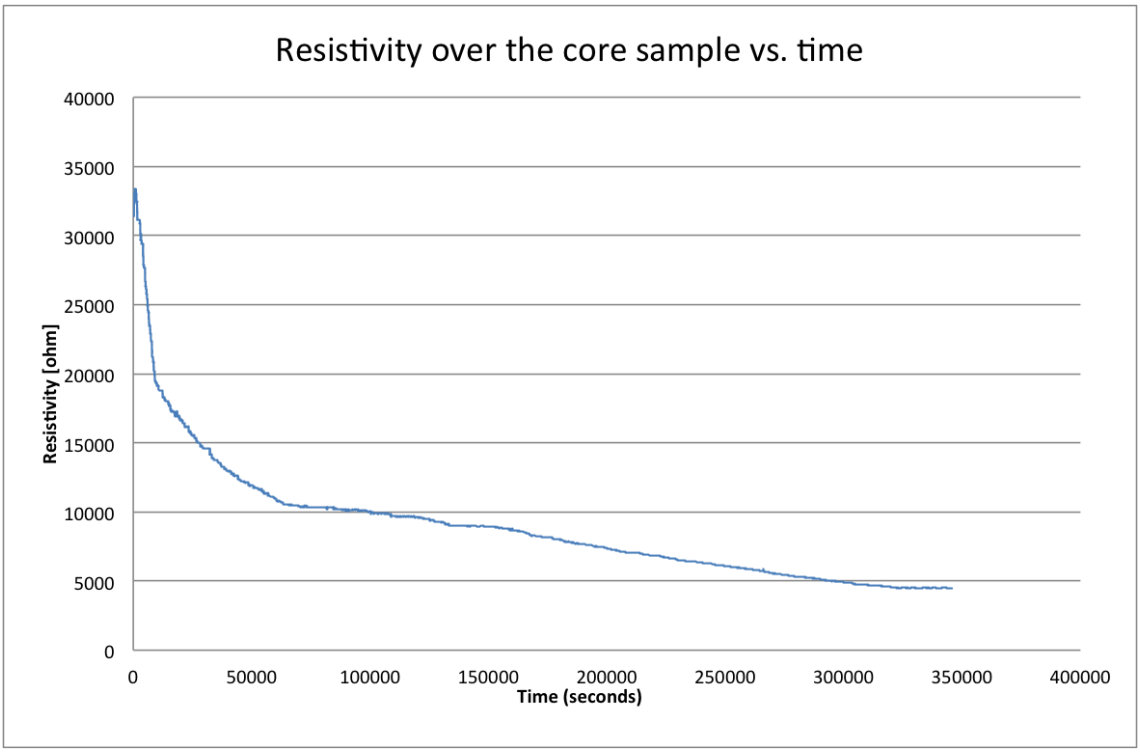

Figure D.3: Resistivity in the water over the core plug, Experiment three.

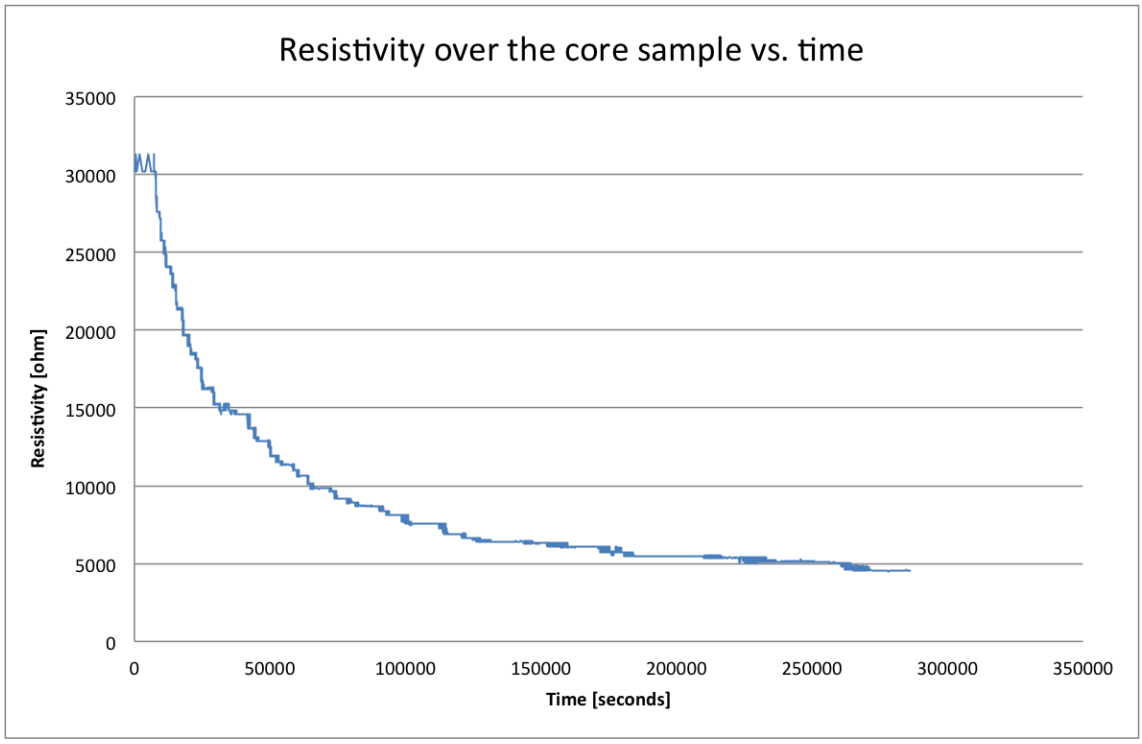

Figure D.4: Resistivity in the water over the core plug, Experiment four.

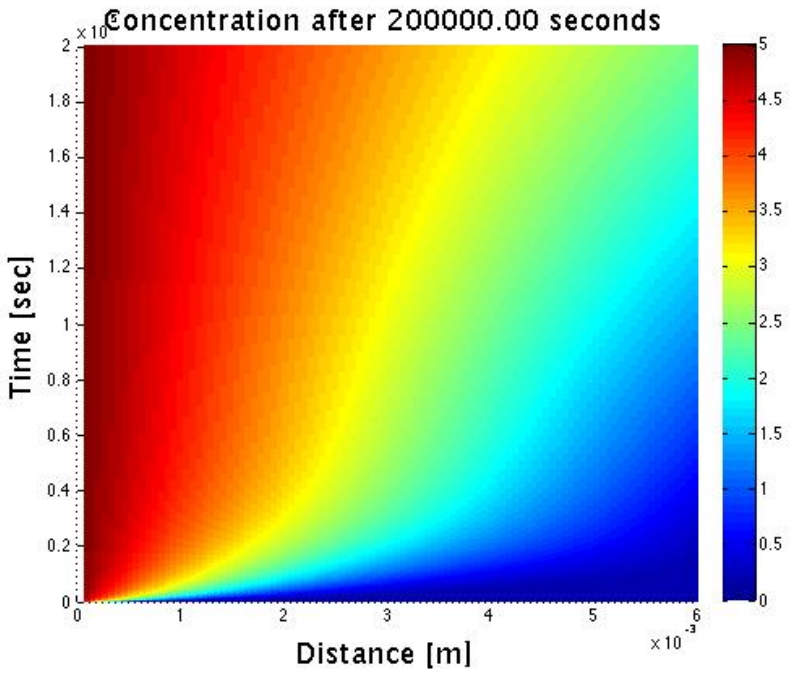

Figure D.5: Concentration of *NaCl* in the water above the core plug in experiment one

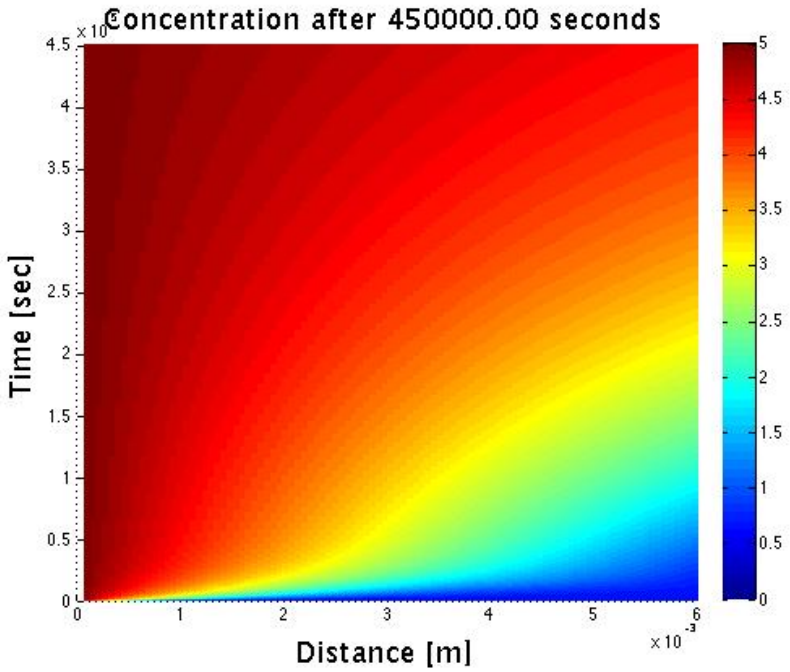

Figure D.6: Concentration of *NaCl* in the water above the core plug in experiment two.

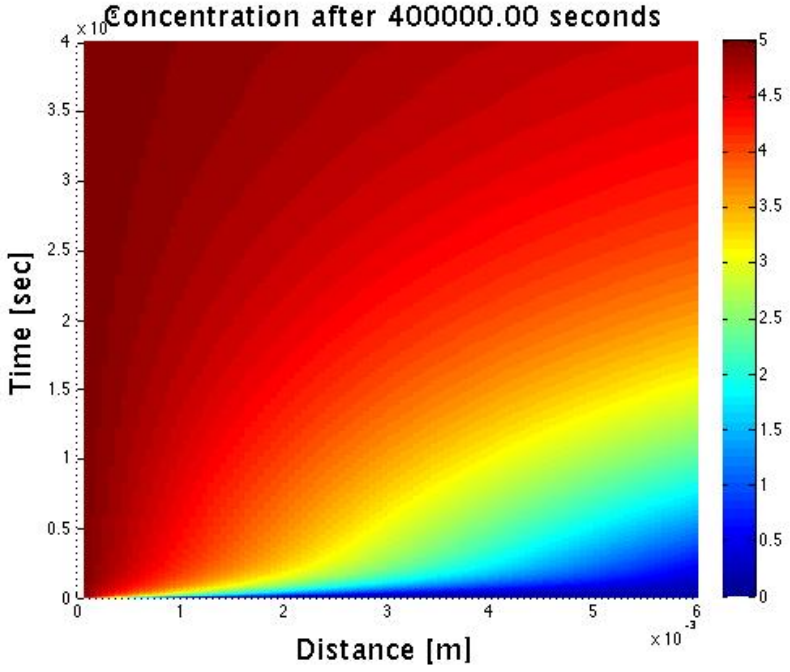

Figure D.7: Concentration of *NaCl* in the water above the core plug in experiment three.

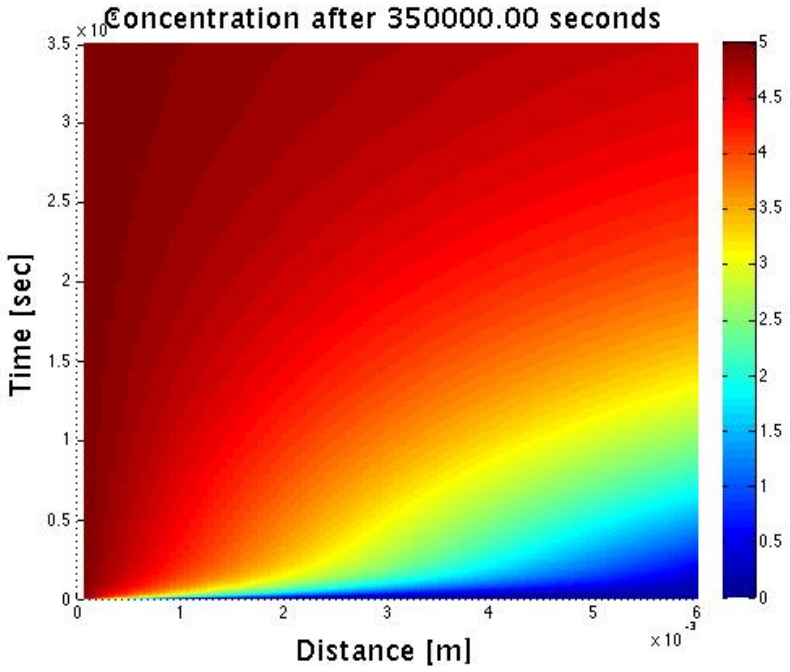

Figure D.8: Concentration of *NaCl* in the water above the core plug in experiment four.

Appendix E

Risk Assessment

ID	20180	**Status**	**Dato**
Risikoområde	Risikovurdering: Helse, miljø og sikkerhet (HMS)	Opprettet	09.05.2017
Opprettet av	Hedda Henriksdatter Blytt	Vurdering startet	09.05.2017
Ansvarlig	Hedda Henriksdatter Blytt	Tiltak besluttet	
		Avsluttet	09.06.2017

Risikovurdering:

An experimental and numerical study of diffusion and electrical conductivity in porous media

Gyldig i perioden:
3/1/2017 - 6/11/2017

Sted:
NTNU - Trondheim

Mål / hensikt
Målet er å sammenligne utregnet formasjons faktor fra diffusjon og fra konduktivitet.

Bakgrunn
En del av masteroppgaven, og risikovurdering må gjennomføres for å få tilgang til laben.

Beskrivelse og avgrensninger

Forutsetninger, antakelser og forenklinger
Denne risikovurderingen er forbeholdt arbeidet som skal utføres på laben.

Vedlegg
[Ingen registreringer]

Referanser
[Ingen registreringer]

Oppsummering, resultat og endelig vurdering

I oppsummeringen presenteres en oversikt over farer og uønskede hendelser, samt resultat for det enkelte konsekvensområdet.

Farekilde: **Saltvann**

Uønsket hendelse: **Søle**

Konsekvensområde: Materielle verdier Risiko før tiltak: Risiko etter tiltak:

Endelig vurdering

Den eneste risikoen i detter eksperimentet er søling av saltvann, og dette vil mest sannsynlig ikke skade noen.

Involverte enheter og personer

En risikovurdering kan gjelde for en, eller flere enheter i organisasjonen. Denne oversikten presenterer involverte enheter og personell for gjeldende risikovurdering.

Enhet /-er risikovurderingen omfatter

- NTNU
- Fakultet for ingeniørvitenskap (IV)
- Institutt for geovitenskap og petroleum

Deltakere

[Ingen registreringer]

Lesere

[Ingen registreringer]

Andre involverte/interessenter

Carl Fredrik Berg
Georg Voss
Roger Overå

Følgende akseptkriterier er besluttet for risikoområdet Risikovurdering: Helse, miljø og sikkerhet (HMS):

Helse	Materielle verdier	Omdømme	Ytre miljø

Oversikt over eksisterende, relevante tiltak som er hensyntatt i risikovurderingen

I tabellen under presenteres eksisterende tiltak som er hensyntatt ved vurdering av sannsynlighet og konsekvens for aktuelle uønskede hendelser.

Farekilde	Uønsket hendelse	Tiltak hensyntatt ved vurdering
Saltvann	Søle	Verneutstyr
	Søle	Opplæring i bruk av utstyr

Eksisterende og relevante tiltak med beskrivelse:

Verneutstyr
Beskytter øyne og hud mot kjemikalier.

Avtrekksskap
ved jobb med løsemidler

Opplæring i bruk av utstyr
[Ingen registreringer]

Risikoanalyse med vurdering av sannsynlighet og konsekvens

I denne delen av rapporten presenteres detaljer dokumentasjon av de farer, uønskede hendelser og årsaker som er vurdert. Innledningsvis oppsummeres farer med tilhørende uønskede hendelser som er tatt med i vurderingen.

Følgende farer og uønskede hendelser er vurdert i denne risikovurderingen:

- **Saltvann**
  - Søle

Detaljert oversikt over farekilder og uønskede hendelser:

Farekilde: Saltvann

Søle utover labbenken.

Uønsket hendelse: Søle

Søle på benk eller gulv.

Sannsynlighet for hendelsen (felles for alle konsekvensområder): **Sannsynlig (3)**

Kommentar:
[Ingen registreringer]

Konsekvensområde: Materielle verdier ***Risiko:***

Vurdert konsekvens: **Liten (1)**

Kommentar: Vask etter deg.

Oversikt over besluttede risikoreduserende tiltak:

Under presenteres en oversikt over risikoreduserende tiltak som skal bidra til å reduseres sannsynlighet og/eller konsekvens for uønskede hendelser.

Detaljert oversikt over besluttede risikoreduserende tiltak med beskrivelse:

Detaljert oversikt over vurdert risiko for hver farekilde/uønsket hendelse før og etter besluttede tiltak